Article

Immunity

Precursor Frequency and Affinity Determine B Cell Competitive Fitness in Germinal Centers, Tested with Germline-Targeting HIV Vaccine Immunogens

Graphical Abstract

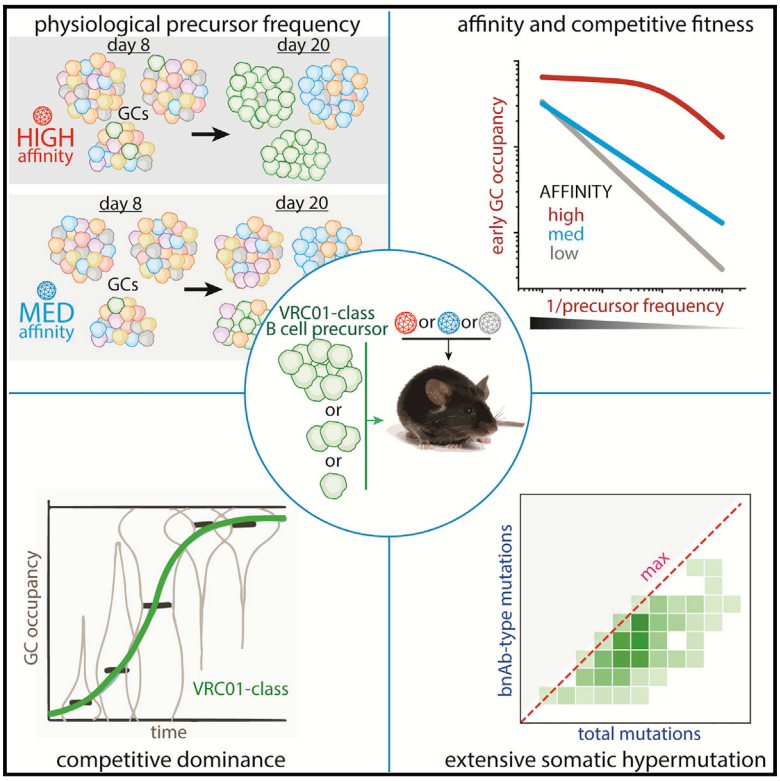

Highlights

- Precursor frequency and affinity limit VRC01-class B cell fitness upon immunization
- Frequency and affinity constraints can be modulated by immunogen multivalency
- Physiologically rare VRC01-class precursor B cells can successfully compete in GCs
- Interclonal competition in germinal centers can resolve within 2–3 weeks

Authors

Robert K. Abbott, Jeong Hyun Lee, Sergey Menis, ..., William R. Schief, David Nemazee, Shane Crotty

Correspondence

schief@scripps.edu (W.R.S.), nemazee@scripps.edu (D.N.), shane@lji.org (S.C.)

In Brief

It is not clear how precursor frequencies and antigen affinities impact interclonal B cell competition. Abbott et al. show these parameters interdependently limit germinal center B cell fitness. When these variables are matched to the human physiological range, HIV bnAb precursor B cells compete in germinal centers, undergo extensive mutation, and form memory.

Abbott et al., 2018, Immunity *48*, 1–14
January 16, 2018
https://doi.org/10.1016/j.immuni.2017.11.023

CellPress

Please cite this article in press as: Abbott et al., Precursor Frequency and Affinity Determine B Cell Competitive Fitness in Germinal Centers, Tested with Germline-Targeting HIV Vaccine Immunogens, Immunity (2017), https://doi.org/10.1016/j.immuni.2017.11.023

Immunity
Article

Precursor Frequency and Affinity Determine B Cell Competitive Fitness in Germinal Centers, Tested with Germline-Targeting HIV Vaccine Immunogens

Robert K. Abbott,[1,2] Jeong Hyun Lee,[1,2] Sergey Menis,[2,3] Patrick Skog,[4] Meghan Rossi,[1,2] Takayuki Ota,[4] Daniel W. Kulp,[2,3,5] Deepika Bhullar,[4] Oleksandr Kalyuzhniy,[2,3] Colin Havenar-Daughton,[1,2] William R. Schief,[2,3,4,6,*] David Nemazee,[4,*] and Shane Crotty[1,2,7,8,*]

[1]Division of Vaccine Discovery, La Jolla Institute for Allergy and Immunology, La Jolla, CA, 92037, USA
[2]Center for HIV/AIDS Vaccine Immunology and Immunogen Discovery (CHAVI-ID), The Scripps Research Institute, La Jolla, CA 92037, USA
[3]IAVI Neutralizing Antibody Center and the Collaboration for AIDS Vaccine Discovery (CAVD), The Scripps Research Institute, La Jolla, CA 92037, USA
[4]Department of Immunology and Microbiology, The Scripps Research Institute, La Jolla, CA 92037, USA
[5]Vaccine and Immune Therapy Center, The Wistar Institute, Philadelphia, PA 19104, USA
[6]Ragon Institute of Massachusetts General Hospital, Massachusetts Institute of Technology, and Harvard University, Cambridge, MA 02139, USA
[7]Division of Infectious Diseases, Department of Medicine, University of California San Diego, La Jolla, CA 92037, USA
[8]Lead Contact
*Correspondence: schief@scripps.edu (W.R.S.), nemazee@scripps.edu (D.N.), shane@lji.org (S.C.)
https://doi.org/10.1016/j.immuni.2017.11.023

SUMMARY

How precursor frequencies and antigen affinities impact interclonal B cell competition is a particularly relevant issue for candidate germline-targeting HIV vaccine designs because of the *in vivo* rarity of naive B cells that recognize broadly neutralizing epitopes. Knowing the frequencies and affinities of HIV-specific VRC01-class naive human B cells, we transferred B cells with germline VRC01 B cell receptors into congenic recipients to elucidate the roles of precursor frequency, antigen affinity, and avidity on B cell responses following immunization. All three factors were interdependently limiting for competitive success of VRC01-class B cells. In physiological high-affinity conditions using a multivalent immunogen, rare VRC01-class B cells successfully competed in germinal centers (GC), underwent extensive somatic hypermutation, and differentiated into memory B cells. The data reveal dominant influences of precursor frequency, affinity, and avidity for interclonal GC competition and indicate that germline-targeting immunogens can overcome these challenges with high-affinity multimeric designs.

INTRODUCTION

The discovery of a deluge of new HIV broadly neutralizing antibodies (bnAbs) in the last 10 years has brought renewed hope that an antibody-based HIV vaccine is possible (Burton and Hangartner, 2016). Ensuing structural, functional, and ontogenic studies of bnAbs have revealed features of bnAbs that present challenges for vaccine design. These challenges include one or more of the following: *in vivo* rarity of proposed bnAb precursor B cells, autoreactivity, and a requirement of substantial somatic hypermutation (SHM) (Mascola and Haynes, 2013). The concept that a bnAb-based HIV vaccine is possible is predicated on the assumption that most individuals in the human population possess bnAb precursors in their naive B cell repertoire. A corollary assumption is that bnAb-class precursor B cells will not be precluded from participating in a vaccine immune response by their rarity or low affinity while competing with non-bnAb-class B cells. Although the specificities of the human naive B cell repertoire are largely unexplored and most bnAb precursor frequencies remain unknown, VRC01-class naive B cells have recently been determined to be present at a frequency of 1 in ~400,000 B cells with a mean affinity of ~3 μM (Jardine et al., 2016a). These findings provide a benchmark for asking fundamental questions about B cell competition and immunodominance: Are naive B cell precursor frequencies or antigen affinity-limiting factors for their successful participation in germinal center (GC) responses following immunization? If so, what are these limits and which immunization strategies can be employed to overcome them?

These questions do not currently have answers. The literature has highly discordant reference points for biologically relevant B cell precursor frequencies and antigen affinities *in vivo*. When considering the universe of molecular structures that B cells can recognize in conjunction with the ~100 million unique naive B cells in a mouse, it might be expected that the frequency of B cells of any given epitope specificity would be relatively rare. Precursor frequencies have been well established for many T cell epitopes. Naive $CD4^+$ T cells specific for a given epitope are found at a precursor frequency of 1:100,000 –1:1,000,000, with a fairly similar range for naive $CD8^+$ T cells (Jenkins and Moon, 2012). Thus, given that B cell epitopes are generally more complex, the VRC01-class naive B cell frequency of 1:400,000 might be expected to be in the mid- to high-range for a B cell epitope specificity. The only well-established mouse naive

B cell epitope-specific frequency determined by direct binding is a precursor frequency of ~1 in 4,000 for the small molecule hapten 4-hydroxy-3-nitrophenyl acetyl (NP) (Weisel et al., 2016) (other haptens have estimates of 1 in 8,000 to 66,000 [Sigal, 1977]), which is a very high precursor frequency in comparison to T cell precursor frequencies. Naive B cell precursor frequencies for whole proteins are estimated to be 1 in 5,000 to 25,000 for phycoerythrin (PE), allophycocyanin (APC), anthrax PA, and influenza hemagglutinin (Kuraoka et al., 2016; Pape et al., 2011), but epitope-specific precursor frequencies are unknown. Thus, the role of B cell precursor frequencies in epitope-specific B cell responses to proteins requires more investigation.

The complementary topic is the uncertainty surrounding biologically relevant antigen affinities of naive B cells. NP-specific B cells with a monovalent affinity of 2 μM K_D (B1-8i) (Sonoda et al., 1997) are frequently studied, but NP-specific B cells with lower affinities participate in the immune response (Dal Porto et al., 1998). In a study of hen egg lysozyme (HEL), it was observed that antigen affinities did not measurably impact recruitment to GCs; however, the affinity range studied was an ostensibly high-affinity range of 10^{-4} μM to 0.1 μM (Chan et al., 2012; Paus et al., 2006). Unexpectedly, in a later study utilizing HEL affinity conditions of 4 μM K_D, no B cell response was detectable *in vivo* with HEL multimerized on sheep red blood cells, leading to the conclusion that affinities in the micromolar range were biologically irrelevant for a protein epitope (Chan et al., 2012), in contrast to findings with NP. More recently, studies of complex antigens have observed immeasurably low affinities of a significant fraction of GC B cells and non-GC B cells (Di Niro et al., 2015; Kuraoka et al., 2016; Tas et al., 2016). One proposed explaination for this observation is that some B cells were responding to non-native antigen forms (“dark antigen”) (Kuraoka et al., 2016), while another proposal is that naive B cells with immeasurably low affinity for antigen constitute a substantial proportion of the antigen-specific immune response (Di Niro et al., 2015). Thus, antigen affinities that are biologically relevant for priming naive B cells remain unclear, which is problematic for vaccine design and basic understanding of B cell biology.

It is well accepted that avidity plays a role in B cell responses to antigens, and multimeric vaccines are preferred to monomeric vaccines. Nevertheless, the magnitude of the role of avidity is unclear, particularly for GC responses, and it is unknown how aspects of avidity relate to other factors involved in immunodominance.

GCs are the anatomic site in which activated B cells undergo the process of SHM and T follicular helper (Tfh) cell-driven selection in response to immunization or infection, in the Darwinian process of affinity maturation (Crotty, 2014; Eisen, 2014). While immunodominance of non-neutralizing B cell epitopes appears to be a major obstacle in HIV and influenza vaccine designs (Angeletti et al., 2017; Havenar-Daughton et al., 2017), an underlying understanding of the basic biology that governs this hierarchy and interclonal competition is largely unknown. Recent studies have suggested that the process of competition within GCs over time is less stringent than previously thought, reigniting study into the basic biological factors that govern GC B cell fate (Kuraoka et al., 2016; Tas et al., 2016).

VRC01-class bnAbs have garnered particular attention for epitope-directed HIV vaccine design efforts, because VRC01-class bnAbs have been shown to neutralize up to 98% of HIV strains (Huang et al., 2016), and possess a binding modality that is opportune for germline-targeting immunogen design (Jardine et al., 2013; McGuire et al., 2013; Zhou et al., 2010). VRC01-class antibodies bind the HIV envelope (Env) CD4 binding site (CD4bs) by principally relying on VH1-2-derived heavy-chain (HC) complementarity determining region 2 (HCDR2) contacts, rather than the more commonly observed HCDR3 dominant binding (Jardine et al., 2016b; Zhou et al., 2010). Inferred germline-reverted VRC01-class Abs do not measurably bind HIV Env due to the Env glycan shield, among other factors (Zhou et al., 2010). This has necessitated the engineering of immunogens capable of binding inferred germline VRC01-class BCRs, including eOD-GT8 (engineered outer domain germline-targeting version 8) and a 60-subunit nanoparticle form of the same immunogen, eOD-GT8 60-mer (Jardine et al., 2013; Jardine et al., 2015). eOD-GT8 60-mers have been shown to elicit VRC01-class B cell responses in VRC01-class HC transgenic mice (Dosenovic et al., 2015; Jardine et al., 2015; Tian et al., 2016) and human immunoglobulin loci transgenic mice (Sok et al., 2016). eOD-GT8-specific naive B cells have been identified in the human B cell repertoire (Jardine et al., 2016a), and eOD-GT8 60-mers are slated to begin first-in-class germline-targeting vaccine human clinical trials in 2018. A series of structure-based boosting immunogens have been designed, with the goal of shepherding affinity maturation of VRC01-class naive B cells into VRC01-class bnAbs via serial immunizations following a eOD-GT8 60-mer prime (Briney et al., 2016; Jardine et al., 2016b). Proof-of-concept for this approach has been demonstrated for a PGT121-class germline-targeting immunogen series (Escolano et al., 2016; Steichen et al., 2016). However, successful complete maturation of VRC01-class bnAbs to broadly neutralize clinically relevant Tier 2 HIV strains has not yet been achieved by immunization. Mature VRC01-class bnAbs depend on extensive affinity maturation to develop potency and breadth during HIV infection, with 32%–48% mutated amino acids (aa) in most VRC01-class bnAbs (Huang et al., 2016; Scheid et al., 2011). VRC01 affinity maturation additionally depends on a rare deletion event in light chain (LC) CDR1 (LCDR1). These aspects of VRC01-class affinity maturation, plus the rarity of bnAb precursors in the human B cell repertoire, highlight the need for animal models to assess immune responses to germline-targeting immunogens.

RESULTS

Development of a Cell Transfer Model for Investigating VRC01-Class B Cell Responses

We hypothesize that antigen affinity, avidity, and VRC01-class B cell precursor frequency are limiting for B cell activation, competition, and memory formation in humans. However, attempting to directly address this overarching hypothesis in preclinical *in vivo* models is challenging due to the fact that mice, rats, rabbits, and macaques all lack VH1-2 or a comparable VH gene required for VRC01-class antibody responses (Jardine et al., 2013; West et al., 2012; Wu et al., 2011). Human immunoglobulin locus transgenic “Kymab” mice are one available model, but they have an abnormally low VRC01-class precursor B cell frequency; lower than humans by 150- to 900-fold (Sok et al.,

2016). We and others have developed germline-reverted VRC01-class HC (VRC01^{gH}) knock-in mice, which respond to germline-targeting immunogens (Briney et al., 2016; Dosenovic et al., 2015; Jardine et al., 2015; Tian et al., 2016). Although these mouse models are useful tools to assess different immunogen designs, including eOD-GT8 60mers, they are not able to test VRC01-class B cell responses directly at physiologically relevant B cell precursor frequencies. Unimmunized VRC01^{gH} mice possess eOD-GT8 binding B cells at a frequency of ~1 in 100 naive B cells (Figure S1A), with the frequency of VRC01-class precursors estimated to be 1 in 1,250 (Jardine et al., 2015). Similar or higher frequencies are expected in the VRC01^{gL}+VH1-2 mouse model (Tian et al., 2016). By comparison, eOD-GT8 binding B cells are present in the human repertoire at a frequency of 1 in 75,000 naive B cells, with VRC01-class B cells (eOD-GT8 binding VH1-2^{+} B cells possessing a 5 amino acid LCDR3) being present at 1 in 400,000 B cells (Jardine et al., 2016a).

To enable experiments with well-defined VRC01-class precursory frequencies and affinities, we first generated germline VRC01 (gVRC01) HC and LC BCR knockin mice (called VRC01^{gHL}, Figure S1B). B cell development was largely normal, and mature VRC01^{gHL} B cells were present in the periphery (Figure S1C–S1F). Heterozygous VRC01^{gHL} mice had ~33% VRC01-class eOD-GT8-binding B cells, while ~90% of B cells in homozygous VRC01^{gHL} mice bound eOD-GT8 (Figure S1G). Heterozygous VRC01^{gHL} mice were used in all subsequent experiments. Endogenous mouse LCs were also expressed on a high fraction of B cells (Figure S1H), probably because the VRC01 gLC is somewhat underexpressed. Total surface BCR expression was comparable between VRC01^{gHL} and wild-type B cells (Figure S1I). VRC01^{gHL} B cells were highly responsive to antigen stimulation. *In vitro* eOD-GT8 60-mer-stimulated VRC01^{gHL} B cells showed active BCR signaling as measured by rapid pERK induction (Figure 1A and S1J) and calcium flux (Figure S1K). *In vivo*, VRC01^{gHL} B cells underwent significant proliferation by 72 hours after immunization with eOD-GT8 60mers (Figure 1B).

To determine how precursor B cell frequency affects cellular fate, we sought to develop a B cell transfer model in which we could finely control B cell starting frequency and track responder B cells. Therefore, we validated a model in which VRC01^{gHL} CD45.2^{+} B cells were transferred into congenic CD45.1^{+} C57BL/6J hosts to establish reliable precursor frequencies of 1 in 1,000, 1 in 10,000, 1 in 100,000, or 1 in 1,000,000 B cells (Figures S1L–S1O). Host mice were immunized with eOD-GT8 60-mer in alum (Figure 1C). At day 8 post-immunization, VRC01^{gHL} CD45.2^{+} B cells had proliferated in all immunized animals (Figure 1D and S1Q), and the responding cells were VRC01-class based on eOD-GT8 probe binding (Figure 1E). CD4bs-specific antibody responses titrated in accordance with VRC01^{gHL} B cell precursor frequency (Figure 1F).

It was unknown whether interclonal competition in the B cell repertoire plays a significant role in B cell recruitment into GC responses to proteins or complex antigens when B cells are present at physiological precursor frequencies. While > 10% of day 8 GC B cells (GL7^{+}BCL6^{+}) were VRC01^{gHL} in mice with high precursor frequencies ($\geq$1 in 10^4 B cells), the representation of VRC01^{gHL} B cells in GCs was reduced in mice with physiological (human) VRC01^{gHL} precursor frequencies of 1 in 10^6 (Figures 1G–1J and S1P–S1S). GC functionality was normal in all cases, as assessed by IgG1 class switching, Tfh cells, T follicular regulatory (Tfr) cells, and dark and light zone GC B cell phenotypes (Figures S2A–S2H). Thus, the VRC01^{gHL} transfer model provides a setting to evaluate effects of B cell precursor frequencies in the context of a vaccine antigen.

Antigen Affinity and Precursor Frequency Are Limiting for GC Recruitment of B Cells

We previously determined that human naive VRC01-class B cells are found in the B cell repertoire with affinities for eOD-GT8 ranging from ~0.1 μM to >100 μM K_D (Jardine et al., 2016a). It is unknown whether all B cells within that range of affinities for eOD-GT8 will respond to immunization, or whether a certain minimum affinity is required for priming and recruitment into an immune response due to intrinsic BCR signaling limits or interclonal competition. In order to better understand the impact of affinity and precursor frequency on B cell responses to a complex antigen, we next developed an *in vivo* model system with transferred VRC01^{gHL} cells wherein we controlled the affinity of the BCR-antigen interaction by using a set of related immunogens with well-defined affinities for VRC01^{gHL} B cells. eOD-GT5, -GT2, and -GT1 have affinities of approximately 0.5 μM, 14 μM, and 40 μM, respectively, for VRC01^{gHL} (Jardine et al., 2013) (Figures S3A–S3C), representing the range of BCR affinities of naive VRC01-class precursor B cells in humans (Figure 2A). In contrast, the affinity of eOD-GT8 for VRC01^{gHL} is 30 pM.

Immunizations with eOD-GT5, -GT2, or -GT1 60-mer were each able to prime VRC01^{gHL} B cells when VRC01^{gHL} cells were present at a precursor frequency of 1:10^3 – 1:10^4 (a range commonly used in experimental models, which equates to 100–1,000 cells per million B cells), demonstrating that VRC01-class B cells are intrinsically competent to respond *in vivo* to multimerized antigens with affinities at least as low as 40 μM (Figures 2B and 2C). However, under physiological precursor conditions (~1 in 10^6 B cells), the outcomes were dramatically different. Upon eOD-GT2 60-mer or eOD-GT1 60-mer immunization, VRC01^{gHL} GC B cell responses were at or below the limit of detection for 7 of 8 mice ($\leq$0.01% of GC B cells). VRC01^{gHL} B cells were able to mount a GC presence in response to eOD-GT5 60-mer (~1% of GC B cells) (Figure 2C and S3D), representing a ~400-fold increase in cell number from the starting VRC01^{gHL} B cell precursor frequency. Overall, the impact of precursor frequency was nonlinear, as GC occupancy by high affinity VRC01-class B cells dropped only ~10-fold over the same precursor frequency range that resulted in a >100-fold loss of low-affinity responding B cells. Total GC responses were equivalent in all cases (Figures S3E and S3F). We conclude that precursor frequency has a dramatic effect on the competitive fitness of the B cell, as VRC01-class B cells with low affinity were activated and recruited into the GC response when present at a precursor frequency of 1 in 10^3 to 1 in 10^4 but were excluded from the response in most mice when present at the natural precursor frequency of 1 in 10^6. Of note, the frequency of VRC01-class B cells in the human naive B cell repertoire with an affinity of 2 μM or better is approximately 1 in 10^6 (Jardine et al., 2016a). These observations show that GC occupancy by epitope-specific B cells of varying affinities in response to a complex antigen is demonstrably disparate when a high B cell precursor frequency exists in contrast to a low precursor frequency.

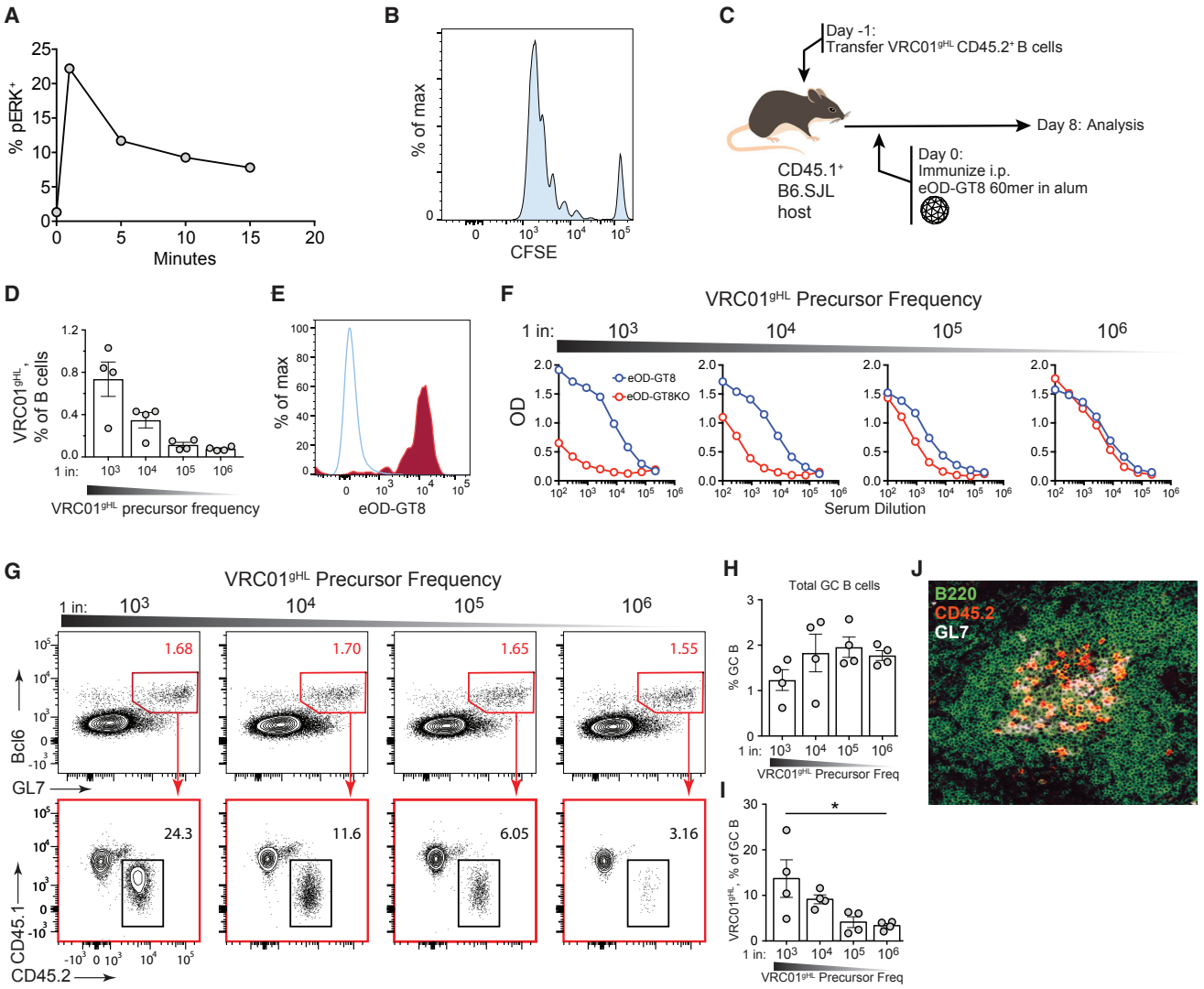

Figure 1. Development of a VRC01^{gHL} B Cell Transfer Model to Assess Precursor Frequency Effects on Immune Responses

(A) pERK induction in VRC01^{gHL} B cells upon stimulation with eOD-GT8 60-mer. n = 3 mice.

(B) 10^6 CFSE-labeled heterozygous VRC01^{gHL} B cells were transferred into CD45.1$^+$ hosts. Host mice were immunized with eOD-GT8 60-mer. Splenocytes were harvested 3 days later and VRC01^{gHL} B cell division was analyzed by flow cytometry. Gated on scatter/singlet/live (SSL), B220$^+$, CD4$^-$, CD45.2$^+$, CD45.1$^-$. n = 3 mice.

(C) Schematic of the VRC01^{gHL} B cell transfer system used for (D)–(J).

(D) Frequency of total VRC01^{gHL} B cells (SSL, CD4$^-$, B220$^+$, CD45.2$^+$, CD45.1$^-$) on day 8 in spleens of mice immunized as in (B), seeded with different VRC01^{gHL} cell precursor frequencies. n = 4 mice/group.

(E) Representative plot of (red) eOD-GT8 60-mer binding to VRC01^{gHL} GC B cells (SSL, CD4$^-$, B220$^+$, CD45.2$^+$, CD45.1$^-$, GL7$^+$, BCL6$^+$) or (blue) naive host B cells (SSL, CD4$^-$, B220$^+$, CD45.2$^-$, CD45.1$^+$, GL7$^-$, BCL6$^-$) on day 8 post-immunization. Host mice were seeded with a 1:10^6 VRC01^{gHL} B cell precursor frequency prior to immunization. n = 4 mice/group.

(F) Representative day 8 serum IgG ELISA data. Blue = WT eOD-GT8 60-mer; Red = CD4bs-KO eOD-GT8 60-mer. n = 4 mice/group.

(G–I) Day 8 GC B cells in mice immunized as in (D). n = 4 mice/group. Representative flow cytometry (G) and quantification (H) of GC B cells. VRC01^{gHL} B cells (CD45.2$^+$) and endogenous B cells (CD45.1$^+$) are indicated within the GC compartment. Pre-gated on SSL, B220$^+$, CD4$^-$. (I) Quantitation of VRC01^{gHL} B cells among GC B cells from G. * = $p < 0.05$. Full gating shown in Figure S1P.

(J) Day 8 spleen GC histology from a host mouse seeded with a 1:10^6 VRC01^{gHL} B cell precursor frequency. Green, B220; red, CD45.2; white, GL7.

Independent Experiments = *E*. (A) *E* = 3; (C) *E* = 2; (D) *E* = 2; (E) *E* = 2; (F) *E* = 2; (G) *E* = 2; (H) *E* = 2; (I) *E* = 2; (J) *E* = 2. Data from one experiment are shown in each panel. See also Figures S1 and S2. Error bars are SEM.

Antigen Multimerization Affects B Cell Competition

Avidity clearly impacts B cell responsiveness to antigen. However, there is little quantitative knowledge of the impact of avidity on B cell responses *in vivo* for monomeric proteins compared to a multimeric form of the same protein. To directly test this under physiological affinities and frequencies, we immunized mice containing either high or low VRC01^{gHL} B cell precursor frequencies with monomeric eOD-GT8, -GT5, and -GT2. Absolute GC

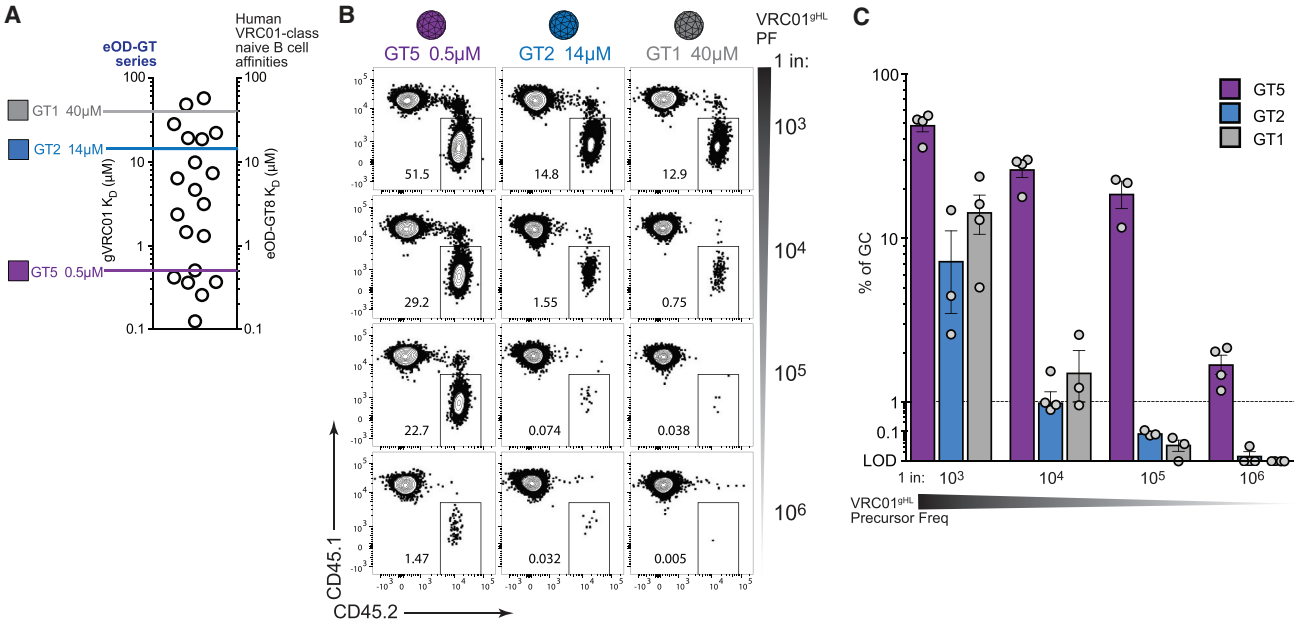

Figure 2. Antigen Affinity and Precursor Frequency Are Limiting for Early GC Occupancy by VRC01^{gHL} B Cells

(A) Relative monovalent affinities of gVRC01 for eOD-GT1 (GT1), eOD-GT2 (GT2), and eOD-GT5 (GT5) monomers (left axis, "eOD-GT series"), in comparison to affinities of human naive B cell VRC01-class Abs for eOD-GT8 (right axis and data points, "Human naive VRC01-class B cell affinities"). Human B cell data points from (Jardine et al., 2016a).

(B) Frequency of VRC01^{gHL} B cells among GC B cells on day 8 following immunization of host mice with eOD-GT1, -GT2, or –GT5 60-mer nanoparticles. Host mice started with the different VRC01^{gHL} precursor frequencies (PF) indicated. GC B cells gated as SSL, B220^{+}, CD4^{-}, BCL6^{+}, GL7^{+}. LOD = limit of detection (see STAR Methods for calculations). Each immunogen shown was conducted as an independent experiment. n = 3–4 mice/group.

(C) Quantification of VRC01^{gHL} B cells among GC B, as gated in B. See methods for additional details. n = 3–4 mice/group.

(B) E = 2; (C) E = 2. Data from one experiment are shown in each panel. See also Figure S3. Error bars are SEM.

frequencies on day 8 for all conditions were reduced compared to high-avidity nanoparticle immunogens (Figures 3A and 3B and S3G, in comparison to Figures S3D–S3F), consistent with the notion that the multimeric state of an antigen impacts immunogenicity. Under picomolar affinity monovalent conditions (GT8), VRC01^{gHL} B cells successfully entered GCs. In contrast, under physiological affinity conditions (GT5 and GT2), VRC01^{gHL} B cells were undetectable in the GC response (Figures 3C and 3D, Figure S3H). Even at a high precursor frequency, VRC01^{gHL} B cells were largely excluded from GCs in eOD-GT2 monomer-immunized mice, and were heavily outcompeted in eOD-GT5 immunized mice, only representing 0.1%–0.2% of the GC B cells. This corresponded to a 200- to 500-fold reduction in VRC01^{gHL} B cell occupancy of the GC response after monomer immunization compared to 60-mer immunization. Thus, antigen multimerization impacts the interclonal competitive fitness of B cells across a large range of affinities.

Interclonal GC B Cell Competitive Fitness Is Strongly Influenced by BCR Affinity

While we observed that VRC01^{gHL} B cells could proliferate and enter GCs under physiological precursor and affinity conditions, it was unclear whether those VRC01^{gHL} GC B cells would be competitive in the GC environment. Given that $\geq$ 98% of the GC response consisted of of non-VRC01-class B cells on day 8 post immunization (Figure 2C), it was reasonable to anticipate that the non-VRC01 B cells might remain dominant. In counterpoint, it was difficult to imagine that there would be many naive B cells with affinities better than 14 μM for a protein epitope. Thus, perhaps the low frequency of VRC01^{gHL} B cells initially present in the GC response was due to their starting rare precursor frequency, but after recruitment to GCs the VRC01^{gHL} cells would outcompete non-VRC01 cells due to their stronger starting affinity.

To better understand interclonal GC B cell competition, we assessed the GC response to eOD-GT5 and -GT2 60-mer over the course of 36 days, starting from physiological precursor frequencies. Substantial GC responses to the 60-mer immunizations were ongoing for greater than 20 days in response to eOD-GT5 and -GT2 (Figures 4A and 4B, Figures S3I–S3K). The fate of VRC01^{gHL} B cells in the GCs in each case was quite different. When mice were immunized with the higher affinity eOD-GT5 60-mer immunogen, VRC01^{gHL} B cells outcompeted most B cells over the course of the GC reaction and reached a peak frequency of ~15% of GC B cells (Figures 4B and 4C). Under lower affinity conditions (GT2), VRC01^{gHL} B cells showed minimal outgrowth among GC B cells (Figures 4B and 4D). When total expansion of VRC01-class B cells was directly compared between mice immunized with either GT5 or GT2 60mers, GT5-immunized mice showed an absolute outgrowth of VRC01^{gHL} B cells of ~4,000-fold (Figure 4E and S3J). In contrast, GT2 immunized mice showed essentially no outgrowth of VRC01^{gHL} B cells beyond day 8 (Figure 4E). The kinetics and absolute magnitude of the overall GC B cell responses to each

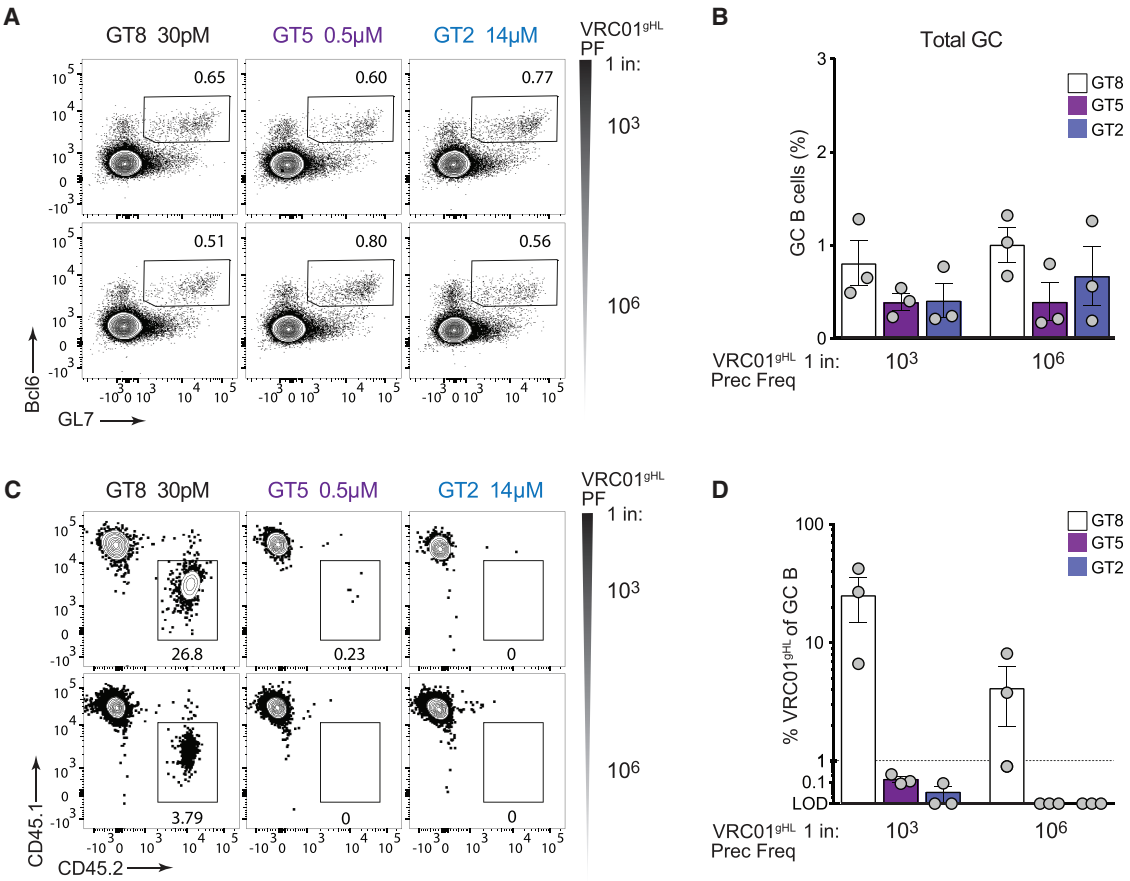

Figure 3. Rare VRC01^{gHL} B Cells Compete Poorly after Monomeric Protein Immunization

(A–D) VRC01^{gHL} B cells were transferred as in Figure 1B to generate CD45.1/VRC01^{gHL} mice with either high (1:10^3 B cells) or low (1:10^6 B cells) precursor frequencies. Mice were immunized with the monomeric eOD-GT proteins indicated.

(A and B) Flow cytometric plots (A) and quantitation (B) of total GC B cells in CD45.1/VRC01^{gHL} mice on day 8 following immunization with the monomeric immunogens indicated. Pre-gated on SSL, B220$^+$, CD4$^-$. n = 3 mice/group.

(C and D) (C) Flow cytometric plots and (D) quantitation of VRC01^{gHL} B cells among GC B cells in CD45.1/VRC01^{gHL} mice on day 8 following immunization with the monomeric immunogens indicated. Pre-gated on SSL, B220$^+$, CD4$^-$, Bcl6$^+$, GL7$^+$. n = 3 mice/group.

(A–D), E = 2. Data from one experiment shown in each panel. See also Figure S3. Error bars are SEM.

immunogen were essentially equal, demonstrating that the endogenous, non-VRC01-class B cell response to GT5 and GT2 nanoparticles was comparable, as expected (Figures 4A and S3I). The endogenous GC B cells in both eOD-GT2 and eOD-GT5 60-mer immunized mice recognized at least two different epitopic sites, the CD4bs recognized by VRC01^{gHL} B cells and an independent non-CD4bs site (Figures 4F–4H), demonstrating that the endogenous response was not dominated by a single clonal family.

To determine the level of diversity in the endogenous B cell response, we analyzed single cell BCR sequences of CD4bs-specific endogenous GC B cells (Figure S4A). The sequences revealed that the endogenous CD4bs epitopic response is highly polyclonal (Figure 4I). The majority of day 8 sequences represented unique BCRs as assessed by paired IG_KV-J and IG_HV-D-J assignments (n = 100) (Figure 4I). Certain IG_KV-J and IG_HV-J pairs were enriched on day 8, indicative of selection (Figures 4I–4K, Figures S4B and S4C). Clonal selection progressed over time, with distinct clonal expansions observed on day 36 (Figure 4J). Changes in the distribution of both V_K and V_H gene usage among CD4bs-specific endogenous GC B cells between days 8 and 36 demonstrated that the antigen-specific endogenous cells were subject to substantial interclonal competition (Figures 4I–4K, Figures S4B and S4C). VH1-15*01 represented ~25% of BCR HC usage on day 8 but was not detected at day 36 (Figure 4L, Figure S4C). Antigen recognition seemed primarily LC driven, as dominance (~50%) of four specific V_K genes was established on day 8, representing a much larger fraction of the CD4bs-specific GC repertoire than the naive B cell repertoire (Figure 4K) (Aoki-Ota et al., 2012). These data revealed that the host B cell response was highly diverse and complex, with large numbers of clones successfully competing with VRC01^{gHL} B cells in response to eOD-GT2 60-mer or eOD-GT5 60-mer. This is consistent with diverse early GC composition to other complex antigens (Kuraoka et al., 2016; Tas et al., 2016). Taken together, the results show a dominant role for antigen affinity in competitive success of VRC01^{gHL} B cells over time within GCs when precursor frequency is matched to that of humans.

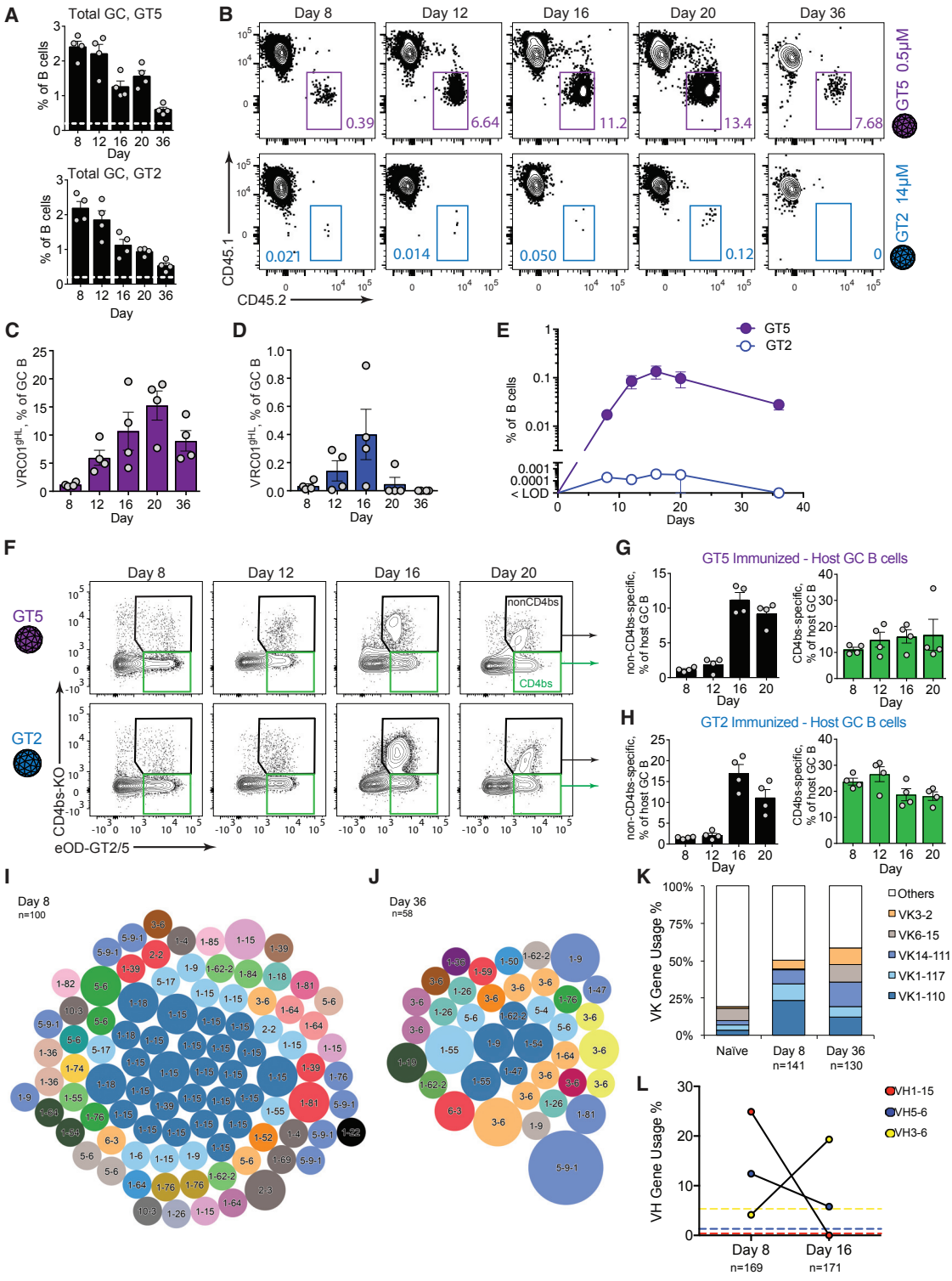

Figure 4. Antigen Affinity Is Limiting for GC Fitness of VRC01^{gHL} B Cells

(A) Frequency of GC B cells over time in eOD-GT5 60-mer (top), or eOD-GT2 60-mer (bottom) immunized CD45.1/VRC01^{gHL} mice, starting with a host mouse VRC01^{gHL} precursor frequency of 1:10^6 B cells prior to immunization. Dotted line represents the average splenic GC B cell frequency in unimmunized controls. n = 4 mice/group.

(B) Flow cytometric plots showing VRC01^{gHL} (CD45.2$^+$) GC B cells and endogenous (CD45.1$^+$, "host") GC B cells among total GC B cells of mice in (A). Cells pre-gated as in Figure 2B. n = 4 mice/group.

(legend continued on next page)

GC Confinement Constrains the Competitive Success of Rare High-Affinity VRC01-Class Precursors

Flow cytometric analysis of GC B cells revealed that rare VRC01^{gHL} B cells expanded to a zenith of ~15% of the response by day 20 after GT5 immunization. To glean spatio-anatomical information on VRC01^{gHL} cell localization and GC occupancy, we performed immunofluorescence staining on spleen cryosections from each time point (Figure 5A and S5A). VRC01^{gHL} B cells were detectable within roughly ~25% of GCs on day 8 (Figures 5A and 5B). At that time point, within any GC positive for VRC01^{gHL} B cells, the VRC01^{gHL} B cell occupancy was generally $\leq$ 10%, indicating that each GC was polyclonal, with endogenous non-VRC01 class B cells making up the vast majority of each individual GC (Figure 5C, S5A). The frequency of GCs populated by VRC01^{gHL} B cells was essentially maintained throughout the course of study, diminishing only slightly by day 36 when few GCs remained (Figure 5B). Strikingly, among GCs positive for VRC01^{gHL} B cells, the VRC01^{gHL} B cells became rapidly dominant over time. Already by day 12, an increase in VRC01^{gHL} B cell occupancy was apparent. By day 16, half of the VRC01^{gHL}-positive GCs were dominated by the VRC01^{gHL} clones, with ~20% of GCs reaching essentially complete exclusion of non-VRC01-class clones. By day 20, the VRC01^{gHL} B cells dominated their GCs, with a median of ~90% occupancy (Figure 5C). These data suggest that, within the parameters used here, interclonal competition can proceed rapidly, with purification of any given GC frequently occurring by day 16–20. Of note, some VRC01^{gHL}-positive GCs remained less than 50% occupied by VRC01^{gHL} B cells. This might reflect the frequency of endogenous B cell clones that have approximately equal affinity to VRC01^{gHL} B cells, or alternatively might reflect stochastic effects on clonal selection and survival in GCs.

Extensive SHM Occurs when Starting from Rare Physiological Precursor Frequencies

Germline-targeting vaccine design is a new concept, not yet tested in humans, or any species under physiological precursor frequency and affinity conditions. The available data have indicated that germline-targeting reductionist design vaccine regimens might need to occur as three phases: a germline-priming phase that amplifies the number of precursor B cells specific for the bnAb epitope, a shepherding phase that utilizes a series of modified immunogens to affinity mature the B cells through SHM to acquire measurable affinity for the pathogen, and a polishing phase that utilizes the authentic pathogen epitope (Jardine et al., 2016b). The possibility that the germline-priming immunization is largely restricted to cell number amplification, and not affinity maturation, is supported by the observation of a median of zero to one mutations in amplified VRC01-class B cells after one eOD-GT immunization of VRC01^{gH} or VRC01^{gL}+VH1-2 mice (Briney et al., 2016; Jardine et al., 2015; Tian et al., 2016). However, as noted in those studies, the precursor frequencies and affinities of precursor B cells were non-physiologically high. That might have blunted GC selection pressure for SHM (Shih et al., 2002). Thus, we assessed whether SHMs were enhanced, unchanged, or reduced under physiological precursor frequency and affinity conditions.

To measure the frequency and characteristics of the SHMs, we performed single cell sorting of VRC01^{gHL} GC B cells from splenocytes obtained at 8, 16, and 36 days following a single eOD-GT5 60-mer immunization of mice with a starting VRC01^{gHL} precursor frequency of 1 in 10^6 B cells, as established above. Both the gVRC01 HC and LC acquired increasing numbers of mutations over time (Figure 6A, Figure S6A, Tables S1 and S2). By day 16, all clones contained at least one aa mutation in the HC, with a median of two mutations (Figure 6A). By day 36, extensive SHM of the HC had occurred, with a median of six HC aa mutations per clone, with again every clone containing at least one aa mutation (Figure 6A, Table S3). Several clones contained > 10aa mutations, representing a HC amino acid mutation frequency of > 9.3% after a single immunization. The LC sequences also exhibited substantial SHM, with ~50% mutated at day 16 and 87% at day 36 (Figure 6A). Several day 36 clones possessed LCs with > 5aa mutations each. The HC was more frequently mutated per residue position compared to the LC (Figure 6B). Thus, extensive SHM of bnAb precursors was observed after one immunization when starting from physiological affinity and precursor frequency conditions.

Mature VRC01-class bnAb mutations can be defined based on known bnAbs. VRC01^{gHL} B cell recipient mice exhibited a strong bnAb directionality to their mutation path, as the majority of the HC SHMs were bnAb-type mutations (Figures 6C–6E, excluding

(C and D) Quantitation of VRC01^{gHL} GC B cells in eOD-GT5 60-mer-immunized mice (C, purple) or eOD-GT2 60-mer-immunized mice (D, blue) as a percentage of total GC B cells. n = 4 mice/group.

(E) Quantitation of VRC01^{gHL} B cells among total B cells in the mice shown in (A)–(D). n = 4 mice/group.

(F) eOD-GT2 or eOD-GT5 and eOD-GT8-CD4bs-KO probe binding by endogenous GC B cells in mice immunized as in (A). Gated as SSL, B220$^+$, CD4$^-$, BCL6$^+$, GL7$^+$, CD45.2$^-$, CD45.1$^+$. n = 4 mice/group.

(G) Quantitation of non-CD4bs-specific (left) and CD4bs-specific (right) endogenous ("host") GC B cell responses in mice immunized with eOD-GT5 60-mer as in (A). Gated as in (F). n = 4 mice/group.

(H) Quantitation of non-CD4bs-specific (left) and CD4bs-specific (right) endogenous ("host") GC B cell responses in mice immunized with eOD-GT2 60-mer as in (A). Gated as in (F). n = 4 mice/group.

(I and J) Distribution of eOD-GT CD4bs-specific HC-LC pairs from endogenous GC B cells on day 8 (I) and day 36 (J). Each circle represents the fraction of BCRs that utilize the same HC V-D-J and LC V-J genes. Circles are colored by VK gene, and are text labeled with the corresponding VH gene. Smallest circle = 1 sequence, largest circle = 7 sequences. V gene color code shown in Figure S4. Day 8 data from GT5 and GT2 were pooled (eOD-GT5 and –GT2 n = 4 mice each). Day 36 data were eOD-GT5 (n = 4 mice). See Figure S4 for additional analysis.

(K) The distribution of unpaired VK gene usage in eOD-GT5 60-mer-immunized mice on day 8 (four mice, VK n = 141) and day 36 (four mice, VK n = 130). The most commonly represented VK genes are shown. VK gene usage in naive C57BL/6J mice is shown for reference.

(L) Change in frequently represented IGHV gene usage in eOD-GT5 60-mer-immunized mice between days 8 (four mice, n = 169 sequences) and 36 (four mice, n = 171). Baseline usage frequency of the listed VH genes in naive C57BL/6J mice (Collins et al., 2015) is shown by the color matched dotted lines.

(A and B) $E = 2$; (C) $E = 2$; (D) $E = 2$; (E) $E = 2$; (F) $E = 2$; (G) $E = 2$; (H) $E = 2$; (I) $E = 2$; (J) $E = 1$. Data from one representative experiment shown in (A)–(H). Aggregated data are shown in (I)–(L). See also Figure S4. Error bars are SEM.

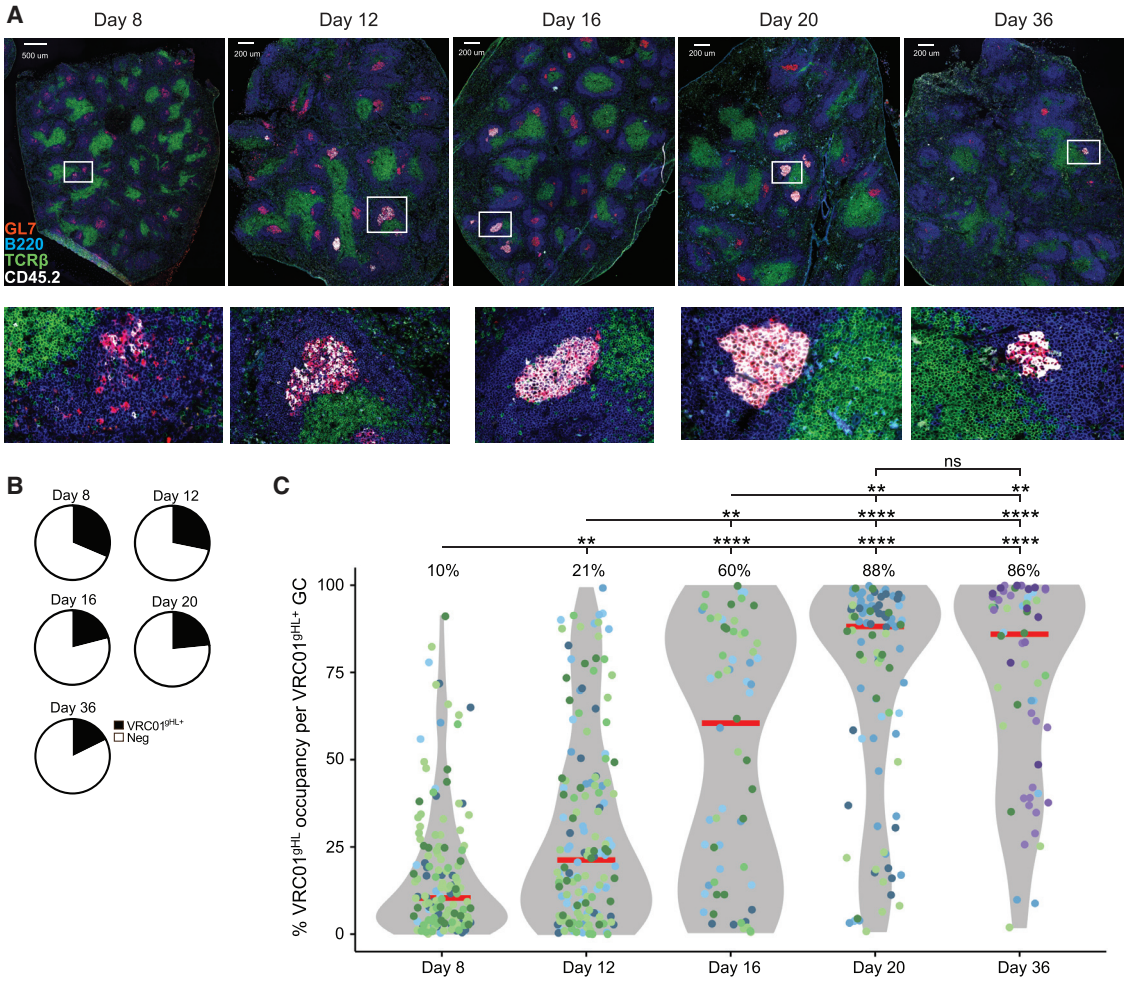

Figure 5. VRC01^{gHL} B Cell Rapidly Dominate Individual GCs under Higher Affinity Conditions

(A) Representative histological images of splenic cryosections from mice immunized with eOD-GT5 60-mer. The day post-immunization is indicated. Host mice VRC01^{gHL} precursor frequency was 1:10^6 B cells prior to immunization. Blue = B220, Green = TCR-β, Red = GL7, White = CD45.2. High magnification images of representative GCs indicated by white boxes are shown below.

(B) The fraction of GCs containing any VRC01^{gHL} B cells (CD45.2$^+$) on the indicated day.

(C) Quantitation of percentage GC occupancy by VRC01^{gHL} B cells (CD45.2$^+$) for each VRC01^{gHL+} GC. Percentage occupancy was calculated based on area. Each dot represents an individual GC. Each shade of color represents an individual mouse. Each color (blue, green, purple) represents an individual experiment. Red bar indicates median percentage VRC01^{gHL} GC occupancy, with number shown above each violin plot. Violin plots show distribution frequencies. Results are pooled from two or three independent experiments (n = 8 total per time point, except d36 where n = 12). Total numbers of GCs analyzed were: d8 = 453, d12 = 598, d16 = 302, d20 = 404, d36 = 254. Numbers of VRC01^{gHL+} GCs assessed for percentage area occupancy by VRC01^{gHL} B cells were: d8 = 153, d12 = 156, d16 = 66, d20 = 105, d36 = 45. ** = $p < 0.01$, and **** = $p < 0.0001$. Additional histology examples shown in Figure S5 for reference.

HCDR3). A progression of mutations was observable from day 8 to 16 to 36 (Figures 6C–6E). By day 36, prominent outgrowth of VRC01^{gHL} cells with 4–5 aa bnAb-type mutations was seen, representing ~60%–80% of total HC aa mutations outside of the HCDR3 in those cells (Figure 6E, Table S3). In two cases, 8 aa bnAb-type mutations were observed. In ~5% of VRC01^{gHL} cells at day 36, all aa SHMs were bnAb-type mutations (Figure 6E). The somatic evolution of the HC was concentrated in HCDR1 and HCDR2, with substantial SHM also present in HCDR3 and the HC framework region 3 (HFWR3) (Figure 6B). Within and around HCDR1, the substitutions at G31, M34, and H35 largely represented bnAb-type mutations (Figures 6F and 6G). Notably, ~82% of HCs acquired the H35N mutation by day 16, and 97% by day 36 (Figure 6G). N35 hydrogen bonds with N100a in HCDR3 of VRC01 (Jardine et al., 2015), and this mutation along with M34L are some of the mutations minimally required in VRC01 (minVRC01) to achieve breadth, most likely via promoting thermodynamic stability between the HCDR1 and HCDR3 loops (Jardine et al., 2016b). In HCDR2, several positions were > 25% mutated (Figure 6B). The important Q61R substitution (Zhou et al., 2010) was present in ~43% of cells by day 36 (Figures 6F and 6G). T57R was in ~36% of cells by day 36 and is specifically observed in the VRC01-class bnAb 12A12. The arginine side chain is in a position that mimics K46 of CD4 (Figure S6B). T57 and G66 HCDR2 positions were heavily mutated and exhibited a high degree of selection (T57R: ~60%, G66D: ~95%) (Figures 6F and

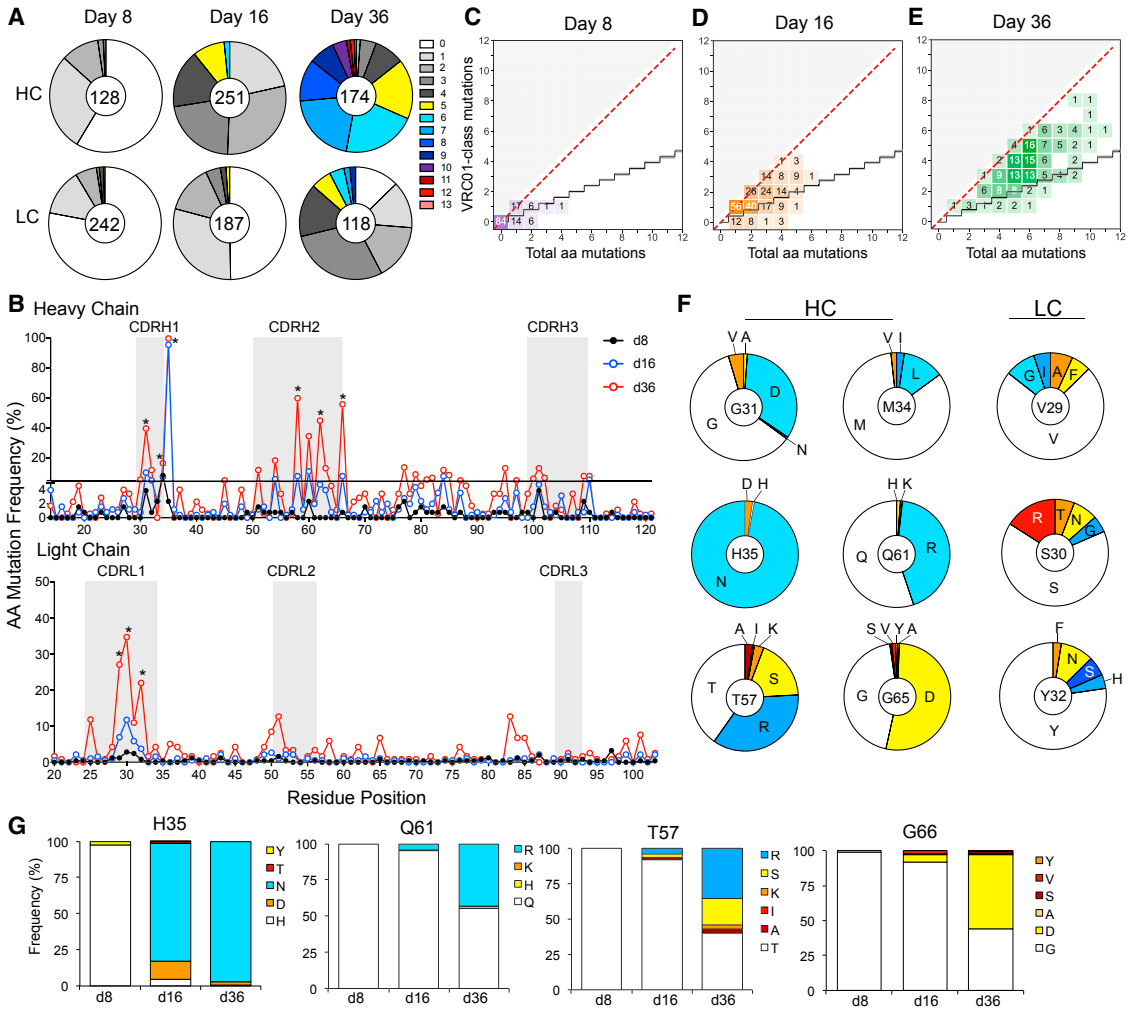

Figure 6. VRC01^{gHL} B Cells Undergo Extensive SHM

(A–G) VRC01^{gHL} BCR sequence data from mice immunized with eOD-GT5 60-mer. Host mice VRC01^{gHL} precursor frequency was 1:10^6 B cells prior to immunization.

(A) Circle charts represent the fraction of HC and LC sequences that acquired the indicated number of aa mutations at day 8, 16, and 36 post-immunization. The total number of individual B cell sequences is shown at the center of the circle.

(B) Frequency of observed HC and LC aa mutations per residue position at day 8, 16, and 36 post-immunization from sequences in (A). Residue positions are listed sequentially. CDRs are highlighted in gray. Asterisks indicate residues analyzed in (F) and (G).

(C–E) bnAb-type aa HC mutations in VRC01^{gHL} B cells from (A and B), shown for d8 (C), d16 (D), and d36 (E). The red diagonal line indicates a 100% efficiency of VRC01-class bnAb-type HC mutations. The black stair step indicates a calculated VH1-2 antigen-agnostic mutation distribution, which might include Ab structure stabilizing mutations. HCDR3 mutations were not included in this analysis, since HCDR sequences vary among different VRC01-class bnAbs.

(F) Circle charts of commonly observed day 36 HC and LC mutations. The aa position (Kabat numbering) and residue in gVRC01 is shown at the center of the circle. VRC01-class bnAb mutations are shown in shades of blue, with the light blue segment representing an exact mutation that occurs in the mature VRC01 bnAb. Non-VRC01-class mutations are colored in shades of yellow and red.

(G) Distribution of select VRC01^{gHL} B cell HC aa mutations over time.

Composite data from all mice are shown in each panel. (A)–(G), day 8, 16, 36 $E = 2$. Day 8, n = 5 mice (HC and LC); day 16, n = 6 mice (HC), n = 5 mice (LC); day 36, n = 4 mice (HC and LC). See also Figure S6 and Tables S1, S2, and S3.

6G), but were not VRC01-class mutations. G66 is distant from both intra-VRC01 and eOD-GT5 contacts and is unlikely to be adjacent to the lumazine synthase core, and thus G66D might stabilize the antibody structure. Overall, a majority of aa mutations that occurred were VRC01-like mutations, demonstrating highly directional somatic evolution.

LCs were less mutated (Figure 6A), with the majority of mutations in LCDR1 (Figure 6B). In VRC01, the LCDR1 provides the majority of LC epitope contacts, interacting with the N276 glycan. This conserved N-linked glycan is the largest structural challenge for the LC (Jardine et al., 2016b; McGuire et al., 2013), but is removed in eOD-GT constructs as a requirement for gVRC01 binding (Jardine et al., 2013). Most VRC01^{gHL} LCDR1 mutations were not recognizable VRC01-class mutations, although we did observe Ser and Gly substitutions that confer loop flexibility (Figure 6F), which might help avoid the N276 glycan (Zhou et al.,

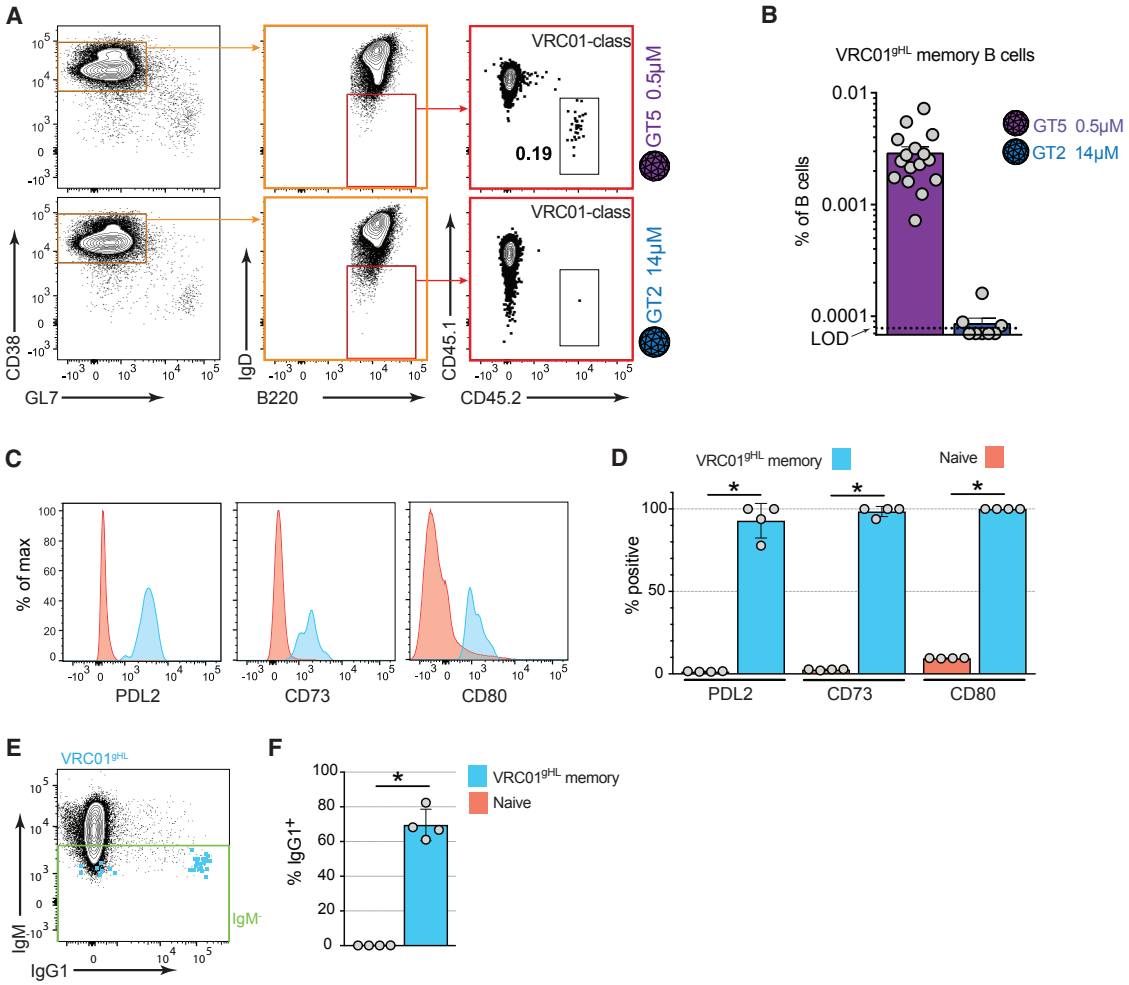

Figure 7. VRC01^{gHL} B Cells Form Memory

(A and B) VRC01^{gHL} memory B cell formation (B220^{+}IgD$^{lo/-}$CD38^{+}GL7^{-}) in CD45.1/VRC01^{gHL} (1:10^{6} precursor frequency) host mice on day 36 following immunization with the immunogens indicated. (A) Representative flow cytometric plots and gating strategy. Prior gating on SSL, B220^{+}, CD4^{-}, CD8^{-}. (B) Quantitation of VRC01^{gHL} memory B cells. LOD = limit of detection (see STAR Methods for calculations). n = 4 mice/group. Data were pooled from 4 (GT5) and 2 (GT2) experiments.

(C) Expression of surface markers on VRC01^{gHL} memory B cells (blue) in eOD-GT5 60-mer immunized mice, gated as in A. Orange, total non-GC B cells (SSL, CD4^{-}, CD8^{-}, B220^{+}, CD38^{+}, GL7^{-}). n = 4 mice/group.

(D) Quantitation of B cells gated as in (C). n = 4 mice/group. *E* = 2.

(E and F) CSR to IgG1 for VRC01^{gHL} memory B cells, in eOD-GT5 60-mer immunized mice, gated as in A. (E) Representative flow cytometry plot, with total endogenous B cells as a black contour plot and VRC01^{gHL} memory B cells overlaid as a blue dot plot. (F) Quantitation of IgG1^{+} memory B cells. n = 4 mice/group. *E* = 2.

See also Figure S6. Error bars are SEM.

2013). Overall, from a single immunization we observed a high frequency of SHM and VRC01 bnAb-type mutations, indicating that a germline-priming immunogen strategy can elicit both clonal amplification and robust directional clonal evolution from rare bnAb precursor B cells with physiologic affinities.

Memory Formation from Rare Precursors Is Unequal and Affinity Dependent

To understand how antigen affinity and precursor frequency affect GC-derived memory B cell formation in a highly competitive system, we assessed VRC01^{gHL} memory B cell development. We found ~30-fold more VRC01^{gHL} memory B cells at day 36 in mice immunized with eOD-GT5 60-mer compared to eOD-GT2 60-mer (Figures 7A and 7B and S6C). VRC01^{gHL} memory B cells were only marginally detectable in eOD-GT2 60-mer immunized mice. To determine whether the memory B cells in GT5 immunized mice were likely to be GC-derived, we assessed class switch recombination and phenotypic memory marker expression by the memory cells (Figures 7C–7F). Class switch recombination within the memory B cell compartment can suggest a GC origin. VRC01^{gHL} memory B cells from eOD-GT5 60-mer-immunized mice were found to be all class switched (~100% IgM^{-}) and predominantly IgG1^{+} (Figures 7E and 7F and S6D). Sevral phenotypic markers have

been utilized to define subsets of memory B cells, including PDL2, CD73, and CD80 (Weisel et al., 2016). Most VRC01^{gHL} memory B cells co-expressed PDL2, CD73, and CD80 (Figures 7C and 7D). Thus, rare VRC01^{gHL} B cells were able to form class-switched memory B cells that were likely to be GC-derived. Nevertheless, antigen affinity within the physiological range was limiting for memory B cell formation in a competitive environment, as eOD-GT2 60-mer immunization elicited far fewer memory B cells.

DISCUSSION

Here we have utilized a new transgenic mouse, a quantitative cell transfer model, and a set of engineered HIV Env germline-targeting immunogens with well-defined affinities for gVRC01 to quantitatively assess roles of precursor frequency, affinity, and avidity on *in vivo* B cell expansion, GC recruitment, GC competition, SHM, and memory B cell development. We showed that the success of an immunogen was sharply dependent on the precursor B cell frequency in the repertoire. At precursor frequencies found in humans, antigen affinity was limiting for the competitive success of VRC01-class B cells. In immunization conditions testing a multivalent immunogen with a physiological high affinity (GT5, ~0.5 μM), rare VRC01-class B cells competed efficiently within GCs, with interclonal competition frequently resolved within 16 days. These VRC01-class B cells underwent extensive affinity maturation, and the memory B cells generated were highly likely to be of GC origin. In addition to clarifying basic features of B cell responses, these findings have implications for vaccine design.

Understanding the impact of precursor frequency was a major goal of this study. Given the universe of B cell paratopes, it would have been reasonable to wager that VRC01-class B cells would outcompete endogenous cells when present at precursor frequencies better than 1 in 100,000 or affinities significantly stronger than 50 μM. However, even at precursor frequencies of 1 in 10,000, VRC01-class B cells failed to dominate the majority of GCs at day 8 under conditions of 40 μM affinity, or even 14 μM affinity. The endogenous B cell data indicated that > 1,000 clones successfully competed with VRC01^{gHL} B cells for GC founding even under GT5 affinity conditions. One possible explanation of these results could be that very low-affinity B cells are recruited to the GC on par with high-affinity cells. However, at physiological precursor frequencies, VRC01^{gHL} B cells were not detectable in GCs under GT1 affinity conditions (or worse affinities. R.A., S.C., unpublished data), and VRC01^{gHL} B cells under 14 μM affinity conditions (GT2) represented less than 0.01% of day 8 GC B cells on average. Thus, a more parsimonious conclusion is that precursor frequency has a major impact on antigen-specific B cell recruitment to GC responses. Consideration of additional data support that conclusion. Testing VRC01^{gHL} B cell responses under a range of precursor frequencies, we observed that from a high precursor frequency a single low-affinity clone could constitute 10% of all GC B cells at day 8, but amount to less than 0.01% of GC B cells when starting from a low precursor frequency. Considering the VRC01^{gHL} cells as representing the equivalent of an epitope-specific class of B cells in a repertoire, these results demonstrate that differences in epitope-specific B cell repertoire frequencies can result in > 1,000-fold differences in the composition of the resulting GC responses.

The finding that precursor frequency and naive BCR affinity for antigen are limiting suggests that both of these variables are important considerations in vaccine design. Based on experiments here, one can suggest that a < 1 μM affinity threshold is a useful target benchmark for successful multivalent germline-targeting immunogen design; that is, if bnAb precursor naive B cells are present at ~1:1,000,000 B cells or better. This is key knowledge, because most epitope-specific HIV bnAb precursor B cells are expected to be rarer than VRC01-class naive B cells. The VRC01^{gHL} B cells might even somewhat underestimate the success rate of rare B cells due to reduced LC expression. Early versus late GC B cell clonal distribution data from NP hapten models (Furukawa et al., 1999), and pathogen proteins (Kuraoka et al., 2016), are consistent with the overall differential precursor frequency model described here. In a monomeric immunization, our data indicate that far higher precursor frequencies and affinities would be required. Under GT5 60-mer conditions, the VRC01-class B cells outcompeted other B cells within individual GCs. Purifying selection in the majority of GCs was accomplished within approximately 16 days. We saw no compelling evidence of stochasticism playing a major role in interclonal GC competition, though our data do not exclude such a role. Affinity appeared to play dominant roles in GC dynamics, as VRC01^{gHL} cells consistently dominated the GCs they seeded under GT5 60-mer conditions, while under GT2 conditions VRC01^{gHL} cells were consistently outcompeted by non-VRC01-class endogenous B cells.

Our data show that germline-targeting can facilitate not only recruitment of B cells but also extensive SHM and directional evolution in response to a single immunization under physiological conditions. Substantially more SHM was observed in this study than in earlier pioneering germline bnAb knockin mouse studies. One possible explanation might be the higher precursor frequencies and affinities utilized, as noted in those studies. B1-8 BCR knockin mice specific for the hapten NP, which have abnormally high precursor B cell frequencies, display impaired affinity maturation (Le et al., 2008). The data here, using more physiological conditions, suggest that germline-targeting vaccine designs can accomplish many cycles of clonal selection and affinity maturation of bnAb precursor B cells after a single immunization. This observation is encouraging, as it might influence future immunogen design and suggests that an effective HIV bnAb immunization protocol might be achieved after a realistic number of immunization "shepherding" steps.

Memory B cell formation was dependent on antigen affinity when B cells were primed under physiological precursor frequencies. In eOD-GT5 60-mer immunized mice, VRC01^{gHL} B cells expanded from a naive precursor frequency of 1 in ~1,000,000 B cells to a memory B cell frequency of 1 in ~35,000 B cells, but in eOD-GT2 60-mer immunized mice VRC01^{gHL} memory B cells reached a barely detectable 1 in ~1,175,000 frequency, highlighting the importance of these variables for memory B cell differentiation. Furthermore, our analysis suggests the majority of the VRC01^{gHL} memory B cells detected in both cases were likely of GC origin.

Taken together, the data show that interdependent roles of precursor frequency, antigen affinity, and avidity control major

aspects of B cell recruitment, GC competition, and GC and memory B cell development.

STAR★METHODS

Detailed methods are provided in the online version of this paper and include the following:

- KEY RESOURCES TABLE
- CONTACT FOR REAGENT AND RESOURCE SHARING
- EXPERIMENTAL MODEL AND SUBJECT DETAILS
  - Mice and Immunizations
- METHOD DETAIL
  - Immunogen Production
  - Histological Analysis
  - ELISAs
  - Flow Cytometry
  - B Cell Transfer
  - BCR Sequencing
- QUANTIFICATION AND STATISTICAL ANALYSIS
  - Statistical Analysis and Calculation of Limit of Detection
  - B Cell Diversity Estimation and Analysis
- DATA AND SOFTWARE AVAILABILITY

SUPPLEMENTAL INFORMATION

Supplemental Information includes six figures, three tables, and Supplemental Experimental Procedures and can be found with this article online at https://doi.org/10.1016/j.immuni.2017.11.023.

ACKNOWLEDGMENTS

We would like to thank the members of the FACS and microscopy facilities at LJI (C. Kim, D. Hinz, L. Nosworthy, R. Simmons, Z. Mikulski, S. McArdle, and A. Lamberth) for outstanding expertise. This work was funded by NIH NIAID grants R01 AI124796 (S.C.), CHAVI-ID UM1 AI100663 (S.C., W.R.S.), R01 AI073148 (D.N., W.R.S.), and R01AI12883 (D.N.). RKA was funded by LJI T32 training grant (AI125179). This work was also funded by IAVI with support from USAID, Netherlands MFA, and Bill & Melinda Gates Foundation; a full list of IAVI donors is available at www.iavi.org (W.R.S).

AUTHOR CONTRIBUTIONS

R.K.A., J.H.L., W.R.S., D.N., and S.C. designed experiments. R.K.A., J.H.L., and M.R. performed experiments and analyzed data. S.M., P.S., D.W.K., and O.K. provided critical reagents and mice. T.O., O.K., and C.H.-D. provided supplemental data. D.B. and D.N. designed and generated VRC01^{gL} mice. R.K.A., J.H.L., and S.C. wrote the paper, with input from the other authors. W.R.S., D.N., and S.C. conceived of the study. S.C. supervised the study.

DECLARATION OF INTERESTS

TSRI and IAVI have filed for a patent related to immunogens in this manuscript.

Received: August 24, 2017
Revised: October 12, 2017
Accepted: November 28, 2017
Published: December 26, 2017

REFERENCES

Angeletti, D., Gibbs, J.S., Angel, M., Kosik, I., Hickman, H.D., Frank, G.M., Das, S.R., Wheatley, A.K., Prabhakaran, M., Leggat, D.J., et al. (2017). Defining B cell immunodominance to viruses. Nat. Immunol. *18*, 456–463.

Aoki-Ota, M., Torkamani, A., Ota, T., Schork, N., and Nemazee, D. (2012). Skewed primary Igκ repertoire and V-J joining in C57BL/6 mice: implications for recombination accessibility and receptor editing. J. Immunol. *188*, 2305–2315.

Briney, B., Sok, D., Jardine, J.G., Kulp, D.W., Skog, P., Menis, S., Jacak, R., Kalyuzhniy, O., de Val, N., Sesterhenn, F., et al. (2016). Tailored Immunogens Direct Affinity Maturation toward HIV Neutralizing Antibodies. Cell *166*, 1459–1470.e11.

Burton, D.R., and Hangartner, L. (2016). Broadly Neutralizing Antibodies to HIV and Their Role in Vaccine Design. Annu. Rev. Immunol. *34*, 635–659.

Chan, T.D., Wood, K., Hermes, J.R., Butt, D., Jolly, C.J., Basten, A., and Brink, R. (2012). Elimination of germinal-center-derived self-reactive B cells is governed by the location and concentration of self-antigen. Immunity *37*, 893–904.

Collins, A.M., Wang, Y., Roskin, K.M., Marquis, C.P., and Jackson, K.J. (2015). The mouse antibody heavy chain repertoire is germline-focused and highly variable between inbred strains. Philos. Trans. R. Soc. Lond. B Biol. Sci. *370*, 370.

Crotty, S. (2014). T follicular helper cell differentiation, function, and roles in disease. Immunity *41*, 529–542.

Dal Porto, J.M., Haberman, A.M., Shlomchik, M.J., and Kelsoe, G. (1998). Antigen drives very low affinity B cells to become plasmacytes and enter germinal centers. J. Immunol. *161*, 5373–5381.

Di Niro, R., Lee, S.J., Vander Heiden, J.A., Elsner, R.A., Trivedi, N., Bannock, J.M., Gupta, N.T., Kleinstein, S.H., Vigneault, F., Gilbert, T.J., et al. (2015). Salmonella Infection Drives Promiscuous B Cell Activation Followed by Extrafollicular Affinity Maturation. Immunity *43*, 120–131.

Dosenovic, P., von Boehmer, L., Escolano, A., Jardine, J., Freund, N.T., Gitlin, A.D., McGuire, A.T., Kulp, D.W., Oliveira, T., Scharf, L., et al. (2015). Immunization for HIV-1 Broadly Neutralizing Antibodies in Human Ig Knockin Mice. Cell *161*, 1505–1515.

Doyle-Cooper, C., Hudson, K.E., Cooper, A.B., Ota, T., Skog, P., Dawson, P.E., Zwick, M.B., Schief, W.R., Burton, D.R., and Nemazee, D. (2013). Immune tolerance negatively regulates B cells in knock-in mice expressing broadly neutralizing HIV antibody 4E10. J. Immunol. *191*, 3186–3191.

Eisen, H.N. (2014). Affinity enhancement of antibodies: how low-affinity antibodies produced early in immune responses are followed by high-affinity antibodies later and in memory B-cell responses. Cancer Immunol. Res. *2*, 381–392.

Escolano, A., Steichen, J.M., Dosenovic, P., Kulp, D.W., Golijanin, J., Sok, D., Freund, N.T., Gitlin, A.D., Oliveira, T., Araki, T., et al. (2016). Sequential Immunization Elicits Broadly Neutralizing Anti-HIV-1 Antibodies in Ig Knockin Mice. Cell *166*, 1445–1458, e1412.

Furukawa, K., Akasako-Furukawa, A., Shirai, H., Nakamura, H., and Azuma, T. (1999). Junctional amino acids determine the maturation pathway of an antibody. Immunity *11*, 329–338.

Gotelli, N.J., and Colwell, R.K. (2011). Estimating species richness. In Biological Diversity: Frontiers in Measurement and Assessment, A.E. Magurran and B.J. McGill, eds. (New York: Oxford University Press), pp. 39–54.

Havenar-Daughton, C., Lee, J.H., and Crotty, S. (2017). Tfh cells and HIV bnAbs, an immunodominance model of the HIV neutralizing antibody generation problem. Immunol. Rev. *275*, 49–61.

Huang, J., Kang, B.H., Ishida, E., Zhou, T., Griesman, T., Sheng, Z., Wu, F., Doria-Rose, N.A., Zhang, B., McKee, K., et al. (2016). Identification of a CD4-Binding-Site Antibody to HIV that Evolved Near-Pan Neutralization Breadth. Immunity *45*, 1108–1121.

Jardine, J., Julien, J.P., Menis, S., Ota, T., Kalyuzhniy, O., McGuire, A., Sok, D., Huang, P.S., MacPherson, S., Jones, M., et al. (2013). Rational HIV immunogen design to target specific germline B cell receptors. Science *340*, 711–716.

Jardine, J.G., Ota, T., Sok, D., Pauthner, M., Kulp, D.W., Kalyuzhniy, O., Skog, P.D., Thinnes, T.C., Bhullar, D., Briney, B., et al. (2015). HIV-1 VACCINES. Priming a broadly neutralizing antibody response to HIV-1 using a germline-targeting immunogen. Science *349*, 156–161.

Jardine, J.G., Kulp, D.W., Havenar-Daughton, C., Sarkar, A., Briney, B., Sok, D., Sesterhenn, F., Ereño-Orbea, J., Kalyuzhniy, O., Deresa, I., et al. (2016a). HIV-1 broadly neutralizing antibody precursor B cells revealed by germline-targeting immunogen. Science *351*, 1458–1463.

Jardine, J.G., Sok, D., Julien, J.P., Briney, B., Sarkar, A., Liang, C.H., Scherer, E.A., Henry Dunand, C.J., Adachi, Y., Diwanji, D., et al. (2016b). Minimally Mutated HIV-1 Broadly Neutralizing Antibodies to Guide Reductionist Vaccine Design. PLoS Pathog. *12*, e1005815.

Jenkins, M.K., and Moon, J.J. (2012). The role of naive T cell precursor frequency and recruitment in dictating immune response magnitude. J. Immunol. *188*, 4135–4140.

Kuraoka, M., Schmidt, A.G., Nojima, T., Feng, F., Watanabe, A., Kitamura, D., Harrison, S.C., Kepler, T.B., and Kelsoe, G. (2016). Complex Antigens Drive Permissive Clonal Selection in Germinal Centers. Immunity *44*, 542–552.

Le, T.-v.L., Kim, T.H., and Chaplin, D.D. (2008). Intraclonal Competition Inhibits the Formation of High-Affinity Antibody-Secreting Cells. J. Immunol. *181*, 6027–6037.

Mascola, J.R., and Haynes, B.F. (2013). HIV-1 neutralizing antibodies: understanding nature's pathways. Immunol. Rev. *254*, 225–244.

McGuire, A.T., Hoot, S., Dreyer, A.M., Lippy, A., Stuart, A., Cohen, K.W., Jardine, J., Menis, S., Scheid, J.F., West, A.P., et al. (2013). Engineering HIV envelope protein to activate germline B cell receptors of broadly neutralizing anti-CD4 binding site antibodies. J. Exp. Med. *210*, 655–663.

Pape, K.A., Taylor, J.J., Maul, R.W., Gearhart, P.J., and Jenkins, M.K. (2011). Different B cell populations mediate early and late memory during an endogenous immune response. Science *331*, 1203–1207.

Paus, D., Phan, T.G., Chan, T.D., Gardam, S., Basten, A., and Brink, R. (2006). Antigen recognition strength regulates the choice between extrafollicular plasma cell and germinal center B cell differentiation. J. Exp. Med. *203*, 1081–1091.

Scheid, J.F., Mouquet, H., Ueberheide, B., Diskin, R., Klein, F., Oliveira, T.Y., Pietzsch, J., Fenyo, D., Abadir, A., Velinzon, K., et al. (2011). Sequence and structural convergence of broad and potent HIV antibodies that mimic CD4 binding. Science *333*, 1633–1637.

Shih, T.A., Meffre, E., Roederer, M., and Nussenzweig, M.C. (2002). Role of BCR affinity in T cell dependent antibody responses in vivo. Nat. Immunol. *3*, 570–575.

Sigal, N.H. (1977). The frequency of para-azophenylarsonate and dimethylaminonapthalene-sulfonyl-specific B cells in neonatal and adult BALB/c mice. J. Immunol. *119*, 1129–1133.

Sok, D., Briney, B., Jardine, J.G., Kulp, D.W., Menis, S., Pauthner, M., Wood, A., Lee, E.C., Le, K.M., Jones, M., et al. (2016). Priming HIV-1 broadly neutralizing antibody precursors in human Ig loci transgenic mice. Science *353*, 1557–1560.

Sonoda, E., Pewzner-Jung, Y., Schwers, S., Taki, S., Jung, S., Eilat, D., and Rajewsky, K. (1997). B cell development under the condition of allelic inclusion. Immunity *6*, 225–233.

Steichen, J.M., Kulp, D.W., Tokatlian, T., Escolano, A., Dosenovic, P., Stanfield, R.L., McCoy, L.E., Ozorowski, G., Hu, X., Kalyuzhniy, O., et al. (2016). HIV Vaccine Design to Target Germline Precursors of Glycan-Dependent Broadly Neutralizing Antibodies. Immunity *45*, 483–496.

Tas, J.M., Mesin, L., Pasqual, G., Targ, S., Jacobsen, J.T., Mano, Y.M., Chen, C.S., Weill, J.C., Reynaud, C.A., Browne, E.P., et al. (2016). Visualizing antibody affinity maturation in germinal centers. Science *351*, 1048–1054.

Tian, M., Cheng, C., Chen, X., Duan, H., Cheng, H.L., Dao, M., Sheng, Z., Kimble, M., Wang, L., Lin, S., et al. (2016). Induction of HIV Neutralizing Antibody Lineages in Mice with Diverse Precursor Repertoires. Cell *166*, 1471–1484, e1418.

von Boehmer, L., Liu, C., Ackerman, S., Gitlin, A.D., Wang, Q., Gazumyan, A., and Nussenzweig, M.C. (2016). Sequencing and cloning of antigen-specific antibodies from mouse memory B cells. Nat. Protoc. *11*, 1908–1923.

Weisel, F.J., Zuccarino-Catania, G.V., Chikina, M., and Shlomchik, M.J. (2016). A Temporal Switch in the Germinal Center Determines Differential Output of Memory B and Plasma Cells. Immunity *44*, 116–130.

West, A.P., Jr., Diskin, R., Nussenzweig, M.C., and Bjorkman, P.J. (2012). Structural basis for germ-line gene usage of a potent class of antibodies targeting the CD4-binding site of HIV-1 gp120. Proc. Natl. Acad. Sci. USA *109*, E2083–E2090.

Wu, X., Zhou, T., Zhu, J., Zhang, B., Georgiev, I., Wang, C., Chen, X., Longo, N.S., Louder, M., McKee, K., et al.; NISC Comparative Sequencing Program (2011). Focused evolution of HIV-1 neutralizing antibodies revealed by structures and deep sequencing. Science *333*, 1593–1602.

Zhou, T., Georgiev, I., Wu, X., Yang, Z.Y., Dai, K., Finzi, A., Kwon, Y.D., Scheid, J.F., Shi, W., Xu, L., et al. (2010). Structural basis for broad and potent neutralization of HIV-1 by antibody VRC01. Science *329*, 811–817.

Zhou, T., Zhu, J., Wu, X., Moquin, S., Zhang, B., Acharya, P., Georgiev, I.S., Altae-Tran, H.R., Chuang, G.Y., Joyce, M.G., et al.; NISC Comparative Sequencing Program (2013). Multidonor analysis reveals structural elements, genetic determinants, and maturation pathway for HIV-1 neutralization by VRC01-class antibodies. Immunity *39*, 245–258.

STAR★METHODS

KEY RESOURCES TABLE

REAGENT or RESOURCE	SOURCE	IDENTIFIER
Antibodies		
Mouse monoclonal anti-mouse-CD45.1 BV711 (clone A20)	Biolegend	Cat#: 110739
Mouse monoclonal anti-mouse-CD45.2 FITC or BUV394 (clone104)	Biolegend / BD Biosciences	Cat#: 109806, 564616
Rat monoclonal anti-mouse-CXCR4 Pe-Dazzle594 (clone L267F12)	Biolegend	Cat#:146514
Rat monoclonal anti-mouse-PDL2 PE (clone Ty25)	Biolegend	Cat#:107206
Armenian hamster monoclonal anti-mouse-CD80 BV421 (clone 16-10A1)	Biolegend	Cat#:104726
Rat monoclonal anti-mouse-CD44 BV785 (clone IM7)	Biolegend	Cat#:103059
Rat monoclonal anti-mouse-CD38 Pe-cy7 (clone 90)	Biolegend	Cat#:102718
Rat monoclonal anti-mouse-CD86 BV421 (clone GL1)	BD Biosciences	Cat#:564198
Rat monoclonal anti-mouse-CD73 BV605 (clone Ty/11.8)	Biolegend	Cat#:127215
Rat monoclonal anti-mouse-IgM FITC (clone II/41)	BD Biosciences	Cat#:553437
Rat monoclonal anti-mouse-CXCR5 biotin (clone SPRCL5)	eBioscience	Cat#:13-7185-82
Rat monoclonal anti-mouse-PD-1 BV605 (clone 29F.1A12)	Biolegend	Cat#:135220
Armenian hamster monoclonal anti-mouse-ICOS BB515 (clone C398.4A)	BD Biosciences	Cat#:565880
Rat monoclonal anti-mouse-Bcl6 PE (clone BCL-DWN)	eBioscience	Cat#:12-5453-82
Rat monoclonal anti-mouse-IgG1 BV421 or PECF594 (clone A85-1)	BD Biosciences	Cat#:562580, 562559
Rat monoclonal anti-mouse-B220 Pacific Blue or BUV496 (clone RA3-6B2)	Biolegend / BD Biosciences	Cat#:103227, 564662
Rat monoclonal anti-mouse-CD4 APC/Fire 750 or APC-H7 (clone GK1.5)	Biolegend / BD Biosciences	Cat#:100460, 560181
Rat monoclonal anti-mouse-CD43 FITC (clone S7)	BD Biosciences	Cat#:553270
Rat monoclonal anti-mouse-CD138 BV650 (clone 281-2)	BD Biosciences	Cat#:564068
Rat monoclonal anti-mouse-CD16/32 purified (clone 2.4G2)	BD Biosciences	Cat#:553142
Rat monoclonal anti-mouse-GL7 PE or Percpcy5.5 (clone GL7)	Biolegend	Cat#:144608, 144610
Rat monoclonal anti-mouse-CD8 APC/Fire 750 or BV570 (clone 53-6.7)	Biolegend	Cat#:100766, 100740
Rat monoclonal anti-mouse-CD11b BV570 (clone M1/70)	Biolegend	Cat#:101233
Armenian hamster monoclonal anti-mouse-CD11c BV570 (clone N418)	Biolegend	Cat#:117331
Rat monoclonal anti-mouse-GR1 BV570 (clone RB6-8C5)	Biolegend	Cat#:108431
Rat monoclonal anti-mouse-Mouse Lambda light chain biotin or BV650 (clone RML-42, or clone R26-46)	Biolegend / BD Biosciences	Cat#:407304, 744526
Rat monoclonal anti-mouse-CD21/35 Percp cy5.5 (clone 7E9)	Biolegend	Cat#:123416
Rat monoclonal anti-mouse-CD23 BV421 (clone B3B4)	Biolegend	Cat#:101621
Rat monoclonal anti-mouse-CD19 APC-H7 (clone 1D3)	BD Biosciences	Cat#:560143
Armenian hamster monoclonal anti-mouse-TCRβ FITC (cloneH57-597)	Biolegend	Cat#:109206
Armenian hamster monoclonal anti-mouse-CTLA-4 Pe-Dazzle 594 (clone UC10-4B9)	Biolegend	Cat#:106318
Rat monoclonal anti-mouse-IgD BV510 or BV786 (clone11-26c.a2)	Biolegend or BD Biosciences	Cat#:405723, 563618
Armenian hamster monoclonal anti-mouse-FAS BV510 (clone Jo2)	BD Biosciences	Cat#:563646

(*Continued on next page*)

Continued

REAGENT or RESOURCE	SOURCE	IDENTIFIER
Mouse monoclonal anti-mouse-phospho-ERK	eBioscience	Cat#:12-9109-42
Rat monoclonal anti-mouse-I-A/I-E Alexa700 (clone M5/114.152)	Biolegend	Cat#:107622
Rat monoclonal anti-mouse-Foxp3 PE-cy7 (clone FJK-16s)	eBioscience	Cat#:25-5773-82
Goat anti-mouse-IgM Fab^2	Jackson Imm0075noresearch	Cat#:115-006-020
Goat anti-mouse-mouse IgG Fc HRP	Bethyl Labs	Cat#: A90-131P
Rat monoclonal anti-mouse kappa light chain FITC (clone RMK-45)	Biolegend	Cat#: 409510
Chemicals, Peptides, and Recombinant Proteins		
eOD-GT1 60mer	Produced in house	N/A
eOD-GT2 60mer	Produced in house	N/A
eOD-GT5 60mer	Produced in house	N/A
eOD-GT8 60mer	Produced in house	N/A
eOD-GT2 avi tagged monomer	Produced in house	N/A
eOD-GT5 avi tagged monomer	Produced in house	N/A
eOD-GT8- KO monomer	Produced in house	N/A
eOD-GT8-KO 60mer	Produced in house	N/A
Streptavidin- BV510	Biolegend	Cat#:405234
Streptavidin-BV421	Biolegend	Cat#:405225
Streptavidin-APC	Biolegend	Cat#:405243
Streptavidin-PE	Biolegend	Cat#:405204
Indo-1, AM, cell permeant	Thermo Fisher	Cat# I1203
Critical Commercial Assays		
Anti FITC Microbeads	Miltenyi Biotec	Cat# 130-048-701
QuadroMACS separator	Miltenyi Biotec	Cat# 130-091-051
Dulbecco's PBS with calcium and magnesium	Gibco	Cat# 14040-133
Horse Serum	Hyclone	Cat# SH30074.03
Lot AAJ208263		
Alexa 647 labeling Kit	Invitrogen	A20186
Bir-A biotin-protein ligase standard reaction kit	Avidity Inc	Cat# BirA500
Histopaque-1077	Sigma	Cat# 10771-500ml
CFSE	Invitrogen	Cat#: C34554
LS Column	Miltenyi Biotec	Cat#: 130-042-401
Experimental Models: Organisms/Strains		
Mouse: B6.SJL-*Ptprc*^{a}*pepc*^{b}/BoyJ	The Jackson Laboratory	JAX: 002014
Mouse: $VRC01^{gH}$	Jardine et al., 2015	N/A
Mouse: $VRC01^{gL}$	This Paper	N/A
Mouse: $VRC01^{gH+/-gL+/-}$	This Paper	N/A
Mouse: $VRC01^{gH+/+,\ gL+/+}$	This Paper	N/A
Oligonucleotides		
Primer VRC01 HC reverse: GCTCAGGGAARTAGCCCTTGAC	IDT	Custom ordered
Primer VRC01 LC Reverse: TGGGAAGATGGATACAGTT	IDT	Custom ordered
Primer VRC01 LFWR2: GAAATTGTGTTGACACAGTCTCC	IDT	Custom ordered
Primer VRC01 LCDR3: CGAAGAACTCGTACTGCTGAC	IDT	Custom ordered
Software and Algorithms		
Flowjo X	Treestar	https://www.flowjo.com/
Adobe Illustrator CS6	Adobe	https://www.adobe.com/

(*Continued on next page*)

Continued

REAGENT or RESOURCE	SOURCE	IDENTIFIER
Zen blue	Zeiss	https://www.zeiss.com/microscopy/us/products/microscope-software/zen.html
Image J Fiji	NIH	https://fiji.sc/
Endnote 7 or 8	Clarivate Analytics	http://endnote.com/downloads
Sequencher	Gene Codes Corporation	https://www.genecodes.com/
Prism 7	GraphPad	https://www.graphpad.com/
Microsoft Office	Microsoft	https://www.office.com/
Tableau	Tableau	https://www.tableau.com/
Unipro Ugene	Open source	http://ugene.net/
IMGT/V-quest		http://www.imgt.org/IMGTindex/V-QUEST.php
Thermo Fisher Armadillo High Performance 96 well PCR plate	Thermo Fisher	Cat#AB2396

CONTACT FOR REAGENT AND RESOURCE SHARING

Further information and requests for reagents may be directed to the corresponding author Shane Crotty (shane@lji.org).

EXPERIMENTAL MODEL AND SUBJECT DETAILS

Mice and Immunizations

B6.SJL-*Ptprc*^{a}*pepc*^{b}/BoyJ mice (CD45.1$^{+/+}$) were purchased from the Jackson labs (Bar Harbor ME) and maintained as an internal breeding colony at the La Jolla Institute (LJI). Both male and female mice between 8-12 weeks of age were used for experiments. For any given individual experiment, age and sex were specifically matched. VRC01^{gH} mice were maintained from original colony developed as previously described (Jardine et al., 2013) at both LJI and the Scripps Research Institute (TSRI). VRC01^{gL} mice were made using the gVRC01 sequence that includes the mature VRC01 LCDR3 (Jardine et al., 2016b) and a targeting construct analogous to that previously published for 4E10 (Doyle-Cooper et al., 2013). Neomycin resistance gene cassette was removed by breeding founder mice to Ella-Cre^{+} mice, as described (Doyle-Cooper et al., 2013). To generate VRC01^{gHL} mice, VRC01^{gL} homozygous mice were bred with homozygous VRC01^{gH} mice to ensure the F1 offspring contain one copy of VRC01^{gH} and VRC01^{gL}. Preparations of given immunogens (eOD-GT1, −2, −5, or −8 60mers) were diluted in PBS (200 μg/ml for 100μl/20μg/mouse and mixed at a 1:1 ratio with 100 μl/mouse Alhydrogel 2% (Invivogen)) for at least 20 minutes, and then injected intraperitoneally (i.p) (total volume of 200μl). For monomeric immunizations indicated eOD–GT monomers were given at a dose of 20μg mouse in Alhydrogel exactly as −60-mer formulations were administered. At day of spleen collection, the peritoneal cavity of all immunized mice was inspected for presence of Alum, assuring proper injection of mice. All mouse experiments were done with approval of IACUC committees of both LJI and TSRI.

METHOD DETAIL

Immunogen Production

eOD-GT8, eOD-GT5, eOD-GT2, eOD-GT1 60mers and corresponding monomers were generated as previously described (Jardine et al., 2013; Jardine et al., 2016a). SPR affinities of gVRC01 for eOD-GT5, eOD-GT2, eOD-GT1 determined previously (Jardine et al., 2013) were repeated (Figure S3), as described (Jardine et al., 2015). For flow cytometric probe binding, monomers were biotinylated by BirA enzymatic reaction (Avidity, Inc) with avi site essentially according to the manufacturer's protocol. Knockout probes which lack VRC01 binding were designed and generated analogous to that previously described (Sok et al., 2016). The eOD-GT8-KO used here contained the sequence for eOD-GT8 with mutations N280R, S365L and F371R to ablate VRC01-class binding ("KO2"). Knockout probes for eOD-GT2 and eOD-GT5 (eOD-GT2-KO and eOD-GT5-KO) each contained respective base sequences with the same 3 mutations to ablate VRC01-class binding. These probes were utilized as both monomers and 60mers depending on indicated condition. Biotinylated monomeric probes for fluorescent detection of GC B cells were pre-reacted in independent tubes for at least 20 minutes to molar excess with fluorescently labeled streptavidin (SA-APC and SA-PE). Any free biotin sites were then quenched by addition of excess free biotin. Reagents were then combined with flow cytometry antibodies for staining.

Histological Analysis

Spleens were frozen in Tissue-Tek (Electron Microscopy Sciences) in a liquid nitrogen-cooled bath of 2-methylbutane. At least 3 5 μm-thick cryosections were cut from each spleen from each time point at least 100 um apart in a cryostat set to −22°C. Sections

were then adhered to RT SuperFrost Plus slides (Fisher Scientific), air-dried for 2 hours at RT, and fixed in a 1:1 mixture of acetone and methanol for 10 minutes at −30°C. Sections were rehydrated and blocked in 0.5% BSA/0.1% Tween-20/PBS (stain/wash buffer used in all subsequent steps), treated with Fc block at 1:200 (clone 2.4G2, BD Biosciences), and stained with mAbs at 1:100 each for 2 hours at RT [B220-(BV421) clone RA3-6B2, GL7-(PE), TCRβ-A488 clone H57-597, CD45.2-A647 clone 104] (Biolegend, San Diego CA). Slides were then washed 3 times, mounted in ProLong Gold™ Antifade Mountant (Invitrogen), and imaged using a Zeiss Axio Scan.Z1 slide scanner with Zen acquisition software. ImageJ/Fiji was used for all subsequent analysis. Images were split into the 4 channels described above. A mask file was created for all T cell zones (TCR-β^+ areas > 8,000μm^2) detected in the splenic section and subtracted from the potential area to detect GCs. Then, in the GL7 channel, holes were filled and all $GL7^+$ areas (> 1,000 um^2) were identified as potential GCs. All proposed GCs were then compared to the $B220^+$ areas and manually evaluated as either appropriate or noise. Lastly, in the CD45.2 channel, holes were filled and the exact $CD45.2^+$ percent area, or $VRC01^{gHL}$ cell occupancy, was calculated as a fraction of each identified GC.

ELISAs

Costar plates were coated with 2μg/mL of either WT or CD4bs-KO protein for eOD-GT1, eOD-GT2, eOD-GT5, or eOD-GT8 60mers for one hour at RT in 0.1M carbonate/0.1M bicarbonate buffer. Plates were then blocked for at least 1 hour at RT (0.5% BSA/PBS) and serially diluted serum samples were added for one hour. Anti-mouse IgG-HRP was utilized for detection (Bethyl Labs). Plates were washed between these steps, and subsequently visualized using TMB substrate (Thermo Scientific), stopped using 0.2M H_2SO_4, and read on a Spectramax plate reader.

Flow Cytometry

Single cell suspensions were generated by mechanical dissociation of spleens. Red blood cells were removed by ACK lysis. Cells were prepared in FACS buffer (5% FCS/PBS), enumerated and Fc blocked (clone 2.4G2, BD Biosciences). Cocktails of mAbs from eBioscience, Biolegend and BD Biosciences were added for 30 minutes at 4°C. If appropriate, secondary stains were performed. Cells were then washed and fixed in either Foxp3 fixation kit (eBioscience) or cytofix/cytoperm (BD Biosciences). For pERK experiments, A647 tagged eOD-GT8 60-mer was used as the immunogen (2-10μg/ml) and reported data (Figure 1A) are gated on eOD-GT8 binding B cells. For pERK, cells were stimulated on a heatblock in standard FACS buffer (5% FCS/PBS) and fixed using 5x volume IC fixation buffer (eBioscience) and put on wet ice immediately. Cells were then permeabilized and stained with pERK antibody for 1 hour at RT. For calcium flux assay, $VRC01^{gHL}$ B cells were stimulated with 0.2 mg/ml of indicated eOD 60-mer and Ca^{2+} flux was assessed by Indo fluorescence by measuring the ratio of 405/485nm after UV excitation . Samples were acquired on an LSR Fortessa, LSRII, or FACS Celesta (BD Biosciences). Cell sorting was done on a FACSAria Fusion (BD Biosciences) with single cell setting enabled at high pressure (61.5psi) at low flow rate (~2). Samples were analyzed on Flowjo X (Treestar). For most experiments 1/3 of the spleen was snap frozen for histological analysis, and the remaining was counted and processed for flow cytometry analysis. All samples were counted using a hemocytometer and absolute numbers of cells per spleen were calculated taking in to account the $1/3^{rd}$ used for histology.

B Cell Transfer

Lymphocytes were prepared from spleens of $VRC01^{gHL}$ by density gradient centrifugation (Histopaq, Sigma). $VRC01^{gHL}$ B cells were phenotyped for eOD-GT8 probe binding prior to transfer in each experiment. B cells were purified by negative selection by magnetic depletion using FITC conjugated anti-CD43 (clone S7), anti-FITC microbeads (Miltenyi Biotec), and an LS column (Miltenyi Biotec). Cells were enumerated on a hemocytometer and transferred retro-orbitally (RO) into recipient hosts. All steps were performed in transfer buffer (5% Horse Serum/Dulbecco's PBS (with calcium and magnesium)). All tubes, pipette tips, and syringe needles were pre-coated for at least an hour at room temperature in transfer buffer to minimize cell loss. Mice were rested for approximately 24 hours before immunization. Cells used for transfers were regularly checked for health by using an aliquot for various *in vitro* stimulation assay. For CFSE labeling, purified B cells were reacted with 10μM CFSE for 8 minutes with gentle rocking at room temperature and then quenched with two washes of transfer buffer and enumerated after labeling.

BCR Sequencing

Individual $VRC01^{gHL}$ B cells were sorted from days 8, 16, and 36 post eOD-GT5 60-mer immunization on a FACSAria Fusion (BD Biosciences). GC $VRC01^{gHL}$ B cells were defined as singlet, scatter, live, $CD4^-$, $CD8^-$, $B220^+$, $GL7^+$, $CD38^-$, $CD45.1^-$, $CD45.2^+$. $VRC01^{gHL}$ memory B cells were defined as $GL7^-$, $CD38^+$, $CD45.1^-$, $CD45.2^+$. Single endogenous antigen-specific GC B cells were defined as singlet, scatter, live, $CD4^-$, $CD8^-$, $B220^+$, $GL7^+$, $CD38^-$, $CD45.2^-$, $CD45.1^+$, eOD-GT8-KO2 $tetramer^-$, eOD-GT5 (or eOD-GT2) SA-$tetramer^+$, $IgD^{lo/-}$, $IgG1^+$. Cells were sorted directly into lysis buffer (0.1 M Trizma HCl pH 8 (Sigma), 10 μg/mL Poly(A) (Roche), 500 U/mL RNase inhibitor (New England BioLabs)) and frozen immediately on dry ice. Plates were stored in −80°C until further processing. First strand cDNA synthesis was carried out using SuperScript II Reverse Transcriptase (Invitrogen) according to manufacturer's instructions. The first of the nested PCR reaction was performed as 16 μL reactions with HotStarTaq Master Mix (QIAGEN), using IgG- and IgK-specific primer pools and thermocycling conditions described previously (von Boehmer et al., 2016). For $VRC01^{gHL}$ cells, the forward primers specific to the leader sequence of the VRC01 LC and HC genes were used. The second reaction was carried out using Phusion polymerase (ThermoFisher) according to the protocol previously described in (Jardine et al., 2016a) with mouse-specific primers (von Boehmer et al., 2016). PCR products were run on a 1 or 1.5% agarose

gel to confirm amplification. Wells with bands of the correct size were sent in for Sanger sequencing. HC products were sequenced using the HC reverse primer from the second PCR reaction (5′ GCTCAGGGAARTAGCCCTTGAC). The LC was sequenced using both the forward (5′-GAYATTGTGMTSACMCARWCTMCA) and reverse primers (5′-TGGGAAGATGGATACAGTT) from the second PCR reaction. The VRC01^{gL} LC was sequenced using a VRC01 LFWR2-specific forward primer (5′-GAAATTGTGTTGACACAGTCTCC) and a VRC01 LCDR3-specific reverse primer (5′-CGAAGAACTCGTACTGCTGAC).

Reads were quality-checked and trimmed in Sequencher, and aligned and analyzed using the ClustalO package within the Unipro Ugene software. Mutation frequencies were calculated using the total number of sequenced residues as the denominator. Mouse Ig gene assignments were carried out via IMGT/V-QUEST. Gene usage diversity was visualized using Tableau (Tableau.com). VRC01-like mutation calculations (Figures 6C–6E) were done as in (Briney et al., 2016), including the estimation of antigen-agnostic VH1-2 mutation accumulation. The black stair step line in Figures 6C–6E indicates the calculated rate of VRC01-class mutations observed in VH1-2^{+} BCR sequences from HIV-unexposed humans and can be considered to be an antigen-agnostic background mutation distribution, which may include VH1-2 Ab structure stabilizing mutations.

QUANTIFICATION AND STATISTICAL ANALYSIS

Statistical Analysis and Calculation of Limit of Detection

Unless otherwise noted, unpaired Mann-Whitney-U non-parametric test was used to assess statistical significance. For Figure 5, a Kruskal-Wallis one-way ANOVA was used with a Dunn's multiple comparisons test to determine statistical significance. Violin plots were generated with R/ggplot2. Individual points on graphs represent individual mice, germinal centers, or sequences depending on data type. Statistical calculations were performed in Graphpad Prism unless stated otherwise. The number of replicates and a description of the statistical method are provided in the applicable figure legends. Data were considered statistically significant at * $p < 0.05$, ** $p < 0.01$, *** $p < 0.001$, and **** $p < 0.0001$.

Limits of detection (LOD) were calculated for multiple experiments. For measuring precursor frequency (Figure S1), host mice with no cells transferred were analyzed by flow cytometry where at least as many B cells as were analyzed from mice in our lowest cell transfer group. Use of the low-valency high affinity GT8-3-mer antigen (Jardine et al., 2015)allowed us to specifically detect 1 in 1 million VRC01-class B cells with no detected background, therefore the background was set as the maximum number of B cells screened. For LOD calculations for day 8 detection of VRC01^{gHL} responsese in GCs (Figures 2, 3, 4) we transferred 1000 VRC01^{gHL} B cells and immunized with 'knockout' eOD-GT2-KO or eOD-GT5-KO 60mers, in which VRC01-class binding is ablated. Thus, no VRC01-class B cell response was expected in the CD45.1/VRC01^{gHL} mice immunized with eOD-GT2-KO or eOD-GT5-KO 60mers. We then measured presence of CD45.2^{+} VRC01^{gHL} cells in GCs (scatter, singlet, live, B220^{+}, CD4^{-}, CD38^{-}, GL7^{+}, CD45.2^{+}, CD45.1^{-}) on day 8 following immunization with these two control proteins and measured 1 in 27,601 GC B cells (0.0005% of GC compartment) on average were from CD45.2^{+} VRC01^{gHL} donor mice non-specifically. Therefore the background was set as 0.0005% of the GC. For establishment of flow cytometry LODs for day 36 memory experiments (Figure 7), we transferred 1000 VRC01^{gHL} B cells into mice which received no immunization and the the CD45.1/VRC01^{gHL} mice were then stained on day 36 to determine background level. From these experiments, the samples were gated as as shown in Figure 7A for "memory" B cells. Zero non-specific cells were detected 1.2 million B cells, and thus background was set to be 1 in 1.2 million B cells. Mean memory B cell expansion from precursor frequency for eOD-GT5 60-mer immunized mice in Figure 7 was calculated to be 28.7-fold.

B Cell Diversity Estimation and Analysis

Endogenous BCRs sequenced from eOD-GT5 and eOD-GT2 immunized mice were analyzed by graphing the distribution of 1) paired HC VDJ and LC VJ usage, 2) unpaired HC VDJ usage only, and 3) unpaired LC VJ usage only, due to the fact that not all of the pairing HC sequences were available for a given LC sequence and vice versa. We estimated the early diversity of endogenous B cells using the bias corrected Chao1 formula defined by the following:

$$S_{chao1} = S_{obs} - \left(\frac{n-1}{n}\right)\left(\frac{f_1(f_1-1)}{2(f_2+1)}\right)$$

where Sobs is the total number of observed species, n = total number of observed individuals, f1 = numerbof singletons, and f2 = number of doubletons (Gotelli and Colwell, 2011). The 100 paired HC VDJ-LC VJ sequences shown in Figure 4I were further sorted on the amino acid sequences of LCDR3 and HCDR3, resulting in 4 doubleton populations (accounting for 8 B cells) and 92 singletons. The paired HC/LC data estimate that about ~925 different GC B cell clones are present on day 8 post immunization. In our analysis, we also found that the HC gene usage was much more diverse than that of the light chain (Figure S4C). As analyzing the HC only sequences provided us a much larger dataset to work with (n = 291), we sorted the HC sequences by VDJ genes and HCDR3 amino acid sequences. In the unpaired HC sequences, we observe 1 tripleton, 19 doubletons, and 250 singletons, which upon applying the Chao1 formula results in an estimated diversity of 1821 unique GC B cell clones.

DATA AND SOFTWARE AVAILABILITY

The accession number for the VRC01 BCR sequencing data reported in this paper is at the Github database: https://github.com/jhl-lji/VRC01gHL_sequences.